Title

Spaceflight-Induced Osteoarthritis in Temporomandibular Joint (TMJ), a Non-Weight-Bearing Joint, and Treatment with Bisphosphonate-Modified PEGylated rNELL-1 (BP-NELL-PEG)

Author

Velicu, Diana-Beatrix

Publication Date

2020

Peer reviewed|Thesis/dissertation

UNIVERSITY OF CALIFORNIA

Los Angeles

Spaceflight-Induced Osteoarthritis in Temporomandibular Joint (TMJ), a Non-Weight-Bearing Joint, and Treatment with Bisphosphonate-Modified PEGylated rNELL-1 (BP-NELL-PEG)

A thesis submitted in partial satisfaction of the

requirements for the degree Master of Science

in Oral Biology

by

Diana-Beatrix Velicu

2020

ABSTRACT OF THE THESIS

Spaceflight-Induced Osteoarthritis in Temporomandibular Joint (TMJ),
a Non-Weight-Bearing Joint, and Treatment with
Bisphosphonate-Modified PEGylated rNELL-1 (BP-NELL-PEG)

by

Diana-Beatrix Velicu
Master of Science in Oral Biology
University of California, Los Angeles, 2020
Professor B Chia Soo, Chair

Purpose: Spaceflight induces osteoporosis by mechanical unloading. Interestingly, recent studies report that microgravity also directly affects osteoblasts (OB) and osteoclasts (OC) *in vitro*, by upregulating OC activity and disrupting the OB cytoskeleton. Non-weight-bearing bones, such as those in the temporomandibular joint (TMJ), provide important insight into cellular-level effects of microgravity *in vivo* without confounding changes in load. NELL-1 is a novel osteogenic growth factor, which upon PEGylation (NELL-PEG) demonstrates enhanced pharmacokinetics and promising potential as a systemic therapy for osteoporosis in mice. To test NELL-PEG systemic therapy in spaceflight-induced osteoporosis, we have collaborated with CASIS and NASA through the Rodent Research 5 (RR-5) mission. This study is a branch of the RR-5 mission and, for the first time, focuses on the TMJ to **investigate how space microgravity and NELL-1-based treatment affect non-load-bearing bones *in vivo*.** Methods: To meet the mission's technical demands, we conjugated NELL-PEG with bioinert bisphosphonate as a bone-targeting molecule

(BP-NELL-PEG, or 'BP-NP') to enhance NELL-PEG's pharmacokinetics and safety. Eight-month-old female BALB/c mice (n=10/group) were randomly assigned to 4 groups: (1) Flight + PBS, (2) Flight + BP-NP, (3) Ground + PBS, and (4) Ground + BP-NP. Flight and Ground groups were housed in the International Space Station and the Kennedy Space Center, FL, respectively, for 9 weeks. Mice received 10mg/kg BP-NP or PBS via intraperitoneal injection every 2 weeks. At 9 weeks, TMJ were analyzed with micro-CT and histology. Results: Micro-CT of subchondral bone in the mandibular condyle showed significantly increased BV/TV in Flight + PBS compared to Ground + PBS. BP-NP treatment showed an even greater increase in BV/TV, in both Ground and Flight groups. There were no significant changes in bone mineral density with either flight or BP-NP treatment. Histological analysis revealed pronounced changes in the condyle cartilaginous zones with BP-NP. Most strikingly, BP-NP treatment showed a 3-fold increase in thickness of the calcified hypertrophic zone in Ground and Flight groups. Conclusion: Spaceflight induces subchondral bone changes in the TMJ, a non-weight-bearing joint, suggesting that microgravity has direct effects on OB and OC and site-specific effects on bone. In addition, BP-NP systemic therapy results in striking chondrogenic and osteogenic changes in the TMJ.

The thesis of Diana-Beatrix Velicu is approved.

Renate Lux

Benjamin Wu

Xinli Zhang

B Chia Soo, Committee Chair

University of California, Los Angeles 2020

TABLE OF CONTENTS

1. INTRODUCTION ***1***

1.2 Osteoporosis and Oral Health **1**

1.2 Micro-gravity induced osteoporosis **2**

1.3 Review of temporomandibular joint **3**

1.4 Temporomandibular joint osteoarthritis (TMJ-OA) **4**

1.5 NELL-1 background **5**

1.6 PEGylation of NELL-1 **7**

1.7 Conjugation of NELL-PEG with inactive bisphosphonate (BP) **7**

2. MATERIALS AND METHODS ***8***

2.1 Harvesting Procedure **10**

2.2 Micro-CT Scan and Analysis **10**

2.3 Histology Analysis **11**

2.4 Statistical Analysis **13**

3. RESULTS ***13***

3.1 Spaceflight Microgravity Induced TMJ-OA in the condyles **13**

3.2 Qualitative Results **14**

3.2.1 Bone Analysis Results 14

3.2.2 Cartilage Analysis Results 14

3.3 Quantitative Results..... 14

3.3.1 Bone Mineral Density (BMD) 14

3.3.2 Bone Volume to Total Volume Ratio (BV/TV) 15

3.3.3 Porosity (%) 15

3.3.4 Trabecular Number (Tb.N), Trabecular Thickness (Tb.Th.) and Trabecular Separation (Tb.Sp.) 15

3.3.5 Mandibular Length Measurements Results 16

3.3.6 Histomorphometric Measurements Results 16

4. DISCUSSIONS 17

5. CONCLUSIONS 19

6. STUDY LIMITATIONS 20

7. FUTURE DIRECTIONS 20

FIGURES 22

REFERENCES 36

LIST OF FIGURES AND TABLES

Figure 1. MicroCT ROI

Figure 2. MicroCT threshold selection

Figure 3. Mandibular length measurements landmarks

Figure 4. Histomorphometric analysis protocol

Figure 5. Histomorphometric layer analysis landmarks

Figure 6. Confirmation of TMJ-OA-like changes in the Flight PBS group

Figure 7. Bone analysis results (qualitative)

Figure 8. Cartilage analysis results (qualitative)

Figure 9. MicroCT results for PBS, BP-BSA and BP-NELL-PEG groups

Figure 10. Mandibular length measurements results

Figure 11. Histomorphometric analysis results

Figure 12. Histomorphometric layer analysis results

Figure 13. Representative histology images with approximately labelled hypertrophic zone

Table 1. Experimental groups

ACKNOWLEDGEMENTS

This MS dissertation would not have been possible without the constant support of my friends and mentors from the Oral Biology MS and Orthodontics Residency programs.

First, I would like to thank Dr. Jin-Hee Kwak, Dr. Kang Ting and Dr. Chia Soo for the exceptional mentorship over the past years. Their outstanding expertise and knowledge inspired me to work harder and be committed to excellence. I would like to thank Dr. Renate Lux, Dr. Benjamin Wu, and Dr. Xinli Zhang, who I am honored to have as committee members.

Additionally, I would like to thank Dr. Zhang for the constant feedback, guidance and advice throughout the years, and for his invaluable expertise in data analysis.

My accomplishments are the result of a group effort. I would like to thank all the team members from the Rodent Research 5 mission, current and past members of the Ting-Soo Laboratory for their dedicated support and stimulating discussions. I would like to thank Mr. Timothy Liu for his patience, diligence and exceptional contribution to this project. I would also like to thank Dr. Jiayu Shi, Mr. Luan Tran, Dr. Pin Ha, Dr. Shahin Maram and Mrs. Samantha Lee for their generous help with my experiments. I would also like to thank Dr. Jenny Jaehee Jeon and Dr. Fangming Li for the motivation, camaraderie and love.

Many thanks to Mr. Matthew Dingman in the Oral Biology division for his patience and guidance in handling the administrative work. I would like to thank NIH, AAOF and CASIS for supporting my research (grant number: NIH/NIDCR K08DE026805, NIH/NIAMS R01AR066782, R01AR068835, R01AR061399, UCLA/NIH CTSI UL1TR000124, CASIS GA-2014-154, AAOF's OFDFA and BRA awards and Colgate's CARE award for J.H.K.).

Finally, I would like to thank my love, Dr. Kevin Bibera, and my family for their financial support and unconditional love during my studies. I would not have made it this far without you.

1. INTRODUCTION

1.2 Osteoporosis and Oral Health

Osteoporosis (OP) is a systemic disease that affects over 200 million people around the world, and more than 53 million people in the US alone[1-6]. The biomedical impact of osteoporosis and its complications is massive, and treatment is predicted to cost over $25 billion worldwide by 2025[7-9]. All bones in the body are affected by osteoporosis[10], including mandibular condyles[11-13]. Clinical studies have suggested that bone degeneration is present in mandibular condylar head and bone mineral density (BMD) is significantly decreased[14, 15] in osteoporotic patients. Condylar resorption has been frequently observed in the presence of decreased level of estrogen in postmenopausal women and osteoarthritis of the temporomandibular joint (TMJ-OA)[16, 17]. An additional studiy has analyzed the bone volume and BMD of the condylar bone in 254 postmenopausal female patients, and demonstrated that reduced condylar bone quality is highly correlated with TMJ-OA development[16]. Temporomandibular joint (TMJ) deformations pose a significant reconstructive challenge and contribute to the progression of temporomandibular disorder (TMD) that is reported to affect 100 million working adults and thus account for the second largest musculoskeletal burden in the US alone[18]. Over the past years, several studies have tried to elucidate the relationship between TMD and other joint diseases and degenerative diseases, but still the mechanism is not completely understood. In addition, studies have indicated that the prevalence of TMD is becoming more complex as the age distribution of reported TMD pain is increasingly widespread[19, 20]. Depending on the population, the reported TMD prevalence in children and adolescents ranges from 16-68%[21, 22] and in the aging population it ranges from 20-40%[20, 23].

Various researchers have been devoted to identifying the key mechanism that underlies TMD and its relationship with osteoporosis. Case reports have detected the presence of ankylosis of the TMJ and open bite after long-term use of bisphosphonates[24, 25], being the most commonly used anti-resorptive drug. Additionally, there is a high incidence of developing Osteonecrosis of the Jaw (ONJ) secondary to BP therapy in cancer patients[26, 27]. From the orthodontic perspective, osteoporotic therapy seems to complicate orthodontic treatment by restraining tooth movement and causing degeneration of the TMJ[28].

1.2 Micro-gravity induced osteoporosis

We propose to utilize a spaceflight-induced osteoporosis model in aged mice because it provides four key benefits. (1) Microgravity generates the highest state of osteoporosis that is not reproducible by a single osteoporosis model on the ground. According to the International Osteoporosis Foundation, 1 out of 3 women over 50 will experience fractures due to osteoporosis, just as 1 out of 5 men[29-31]. Studies show that after the age of 50 we lose around 0.5% of bone per year. Strikingly, astronauts lose around 1.5% of bone per month spent in space[32, 33], which is 36 folds more compared to Earth. (2) Another benefit of utilizing a microgravity model for this study is that it allows investigation of key mechanisms for TMJ degeneration in the context of osteoporosis while excluding the factor of estrogen deficiency as a possible confounding factor. (3) Microgravity accelerates the cellular and physiologic effects of aging. (4) Microgravity also directly affects osteoblasts (OB) and osteoclasts (OC) *in vitro*, by upregulating OC activity and disrupting the OB cytoskeleton. Non-weight-bearing bones, such as those in the TMJ, provide important insight into cellular-level effects of microgravity *in vivo* without confounding changes in load. Exposure to microgravity could induce a rapid degeneration in the cell system that mimics aging in older population. Thus it can be considered as an excellent model for degenerative

diseases[34] that also allows us to efficiently study biological process that occurs in normal aging process[34-36].

Previous in vitro studies performed in real microgravity, reported that microgravity increases osteoclast activity by enhancing resorption pit formation[37], while osteoblasts demonstrated reduced proliferation and activity, differentiation and decreased responsiveness[38]. As a consequence, the absence of gravitational forces acts on a cellular level to induce bone loss, through both an increase in bone resorption by osteoclasts and a decrease in osteoblast cellular integrity.

The current study plans to utilize samples collected from our research group's collaborative mission with the Center for the Advancement of Science in Space (CASIS; the sole manager of the International Space Station, US National Laboratory) and NASA, entitled the Rodent Research 5 (RR-5) mission. This mission consists of America's first live-return of animals, Man's very first live-return of drug-treated animals, and most importantly, World's first successful live-return of rodents with zero mortality and physical/psychological morbidity, which would allow high-quality data. The Flight experiment has completed in August 2017, and a multi-team dissection took place in November 2017 to dissect individual organs and appropriately store them for future analyses.

1.3 Review of the temporomandibular joint

The temporomandibular joint (TMJ) is a ginglymoarthroidal joint that is able to have both rotational and translational movements[39]. The TMJ is formed by the mandibular condyles that fit into the mandibular fossae of the temporal bone. Between the two bony structures lies the articular disc. Besides the main structures, nerves, vessels and ligaments are present.

The composition and development of the TMJ is different compared to other weight-bearing joints in the body. As a result, certain diseases might not target the TMJ or affect it

differently. In synovial joints, the articular surfaces are covered by hyaline cartilage. The TMJ, however, is covered by fibrocartilage[40]. One distinctive characteristic of the fibrocartilage is that it contains both type I and type II Collagen, in comparison with the hyaline cartilage, that only contains type II Collagen[41]. Hyaline cartilage is better able to tolerate compressive loading than fibrocartilage, while fibrocartilage is more resistant to sheer forces[42]. Moreover, fibrocartilage is less likely to change with aging, it has a better potential to repair and it is less likely to break down over time. Because of these molecular differences, the TMJ may be targeted differently by various factors such as sex hormones, that can lead to degenerative changes.

An additional difference between the TMJ and other joints is that the mandibular condyles are covered with secondary cartilage compared to other joints that are covered with primary cartilage[43]. Secondary cartilage develops along with bones that are forming through intramembranous ossification following bone formation. In contrast, primary cartilage growth and development begins in the central layer of the epiphyseal growth plate and it is specific to long bones.

1.4 Temporomandibular joint osteoarthritis (TMJ-OA)

Osteoarthritis is a degenerative joint disease that can affect any joint in the body causing severe pain and dysfunction. Temporomandibular joint osteoarthritis (TMJ-OA) is an important subtype in the classification of temporomandibular disorders (TMD). The pathogenesis of the majority of TMJ-OA is multifactorial and complex or unknown. TMJ-OA is characterized by progressive cartilage degradation, subchondral bone remodeling, chronic inflammation of the synovial tissues and pain. The diagnosis of TMJ-OA is mainly based on the on the radiographic morphology of the condyles and articular eminence, including erosive resorption, sclerosis, osteophyte formation, attrition, and cyst-like changes[44].

The correlation between OP and TMJ-OA is controversial and has yet to be determined. OP and OA are both prevalent conditions associated with ageing and female gender[45]. Current studies suggest that each patient affected with one condition must be evaluated individually for the future occurrence of the other disease. The existence of a common genetic factor has been recognized from family studies, as well as the risk of fractures. A recent study performed on human subjects with healthy and osteoarthritic TMJs, suggested that a low condylar bone quality was significantly correlated with TMJ-OA development. Moreover, the condylar bone mineral density (CT HU) and bone volume fraction (BV/TV) can be used together as a potential diagnostic tool for TMJ-OA (both values are decreased in TMJ-OA)[16].

The purpose of this study is to **assess the effects of space microgravity at the condylar level and to evaluate the outcomes of NELL-1 therapy on the TMJ**.

1.5 NELL-1 background

NEL-like molecule-1 (NELL-1) is a unique secretory molecule that was first discovered in human unilateral craniosynosytosis[46-50]. It is a protein that weights 700 kDa and it is recognized as a potent pro-osteogenic and chondrogenic cytokine[46]. Previously, it was reported that the functions of NELL-1 also include suppression of osteoclast activity, increase in mesenchymal stem cell (MSC) numbers, and suppression of adipogenesis[51-53]. In previous findings NELL-1 was shown to be a direct downstream effector of the osteogenic transcription factor Runt-related transcription factor-2 (Runx2)[54]. Mechanistically, it binds to Integrin β1 and CNTNAP 4 receptors and activates the Wnt/β-catenin signaling pathway[55]. Exogenous NELL-1 promotes robust bone formation in various animal models including femoral[56], calvarial defect[54], and spinal fusion models in rodents and sheep[57-60]. An association between NELL-1 and osteoporosis was also described in a genome-wide linkage study that identified NELL-1 polymorphisms in patients with

reduced BMD[61]. The newly discovered protective function against osteoporosis led us to pursue the therapeutic use of human recombinant (r)NELL-1 for the reversal of osteoporosis[62, 63]. An intramedullary injection model of local NELL-1 treatment in ovariectomized (OVX) rats and sheep showed increased endosteal and trabecular bone formation[62, 63]. Meanwhile, systemic (intravenous) NELL-1 administration reversed OVX-induced osteoporotic bone loss in mice[62]. These findings led us to examine the effects of systemically administered NELL-1-based therapy on spaceflight-induced bone loss, which is reported to be 10 folds greater than osteoporosis observed in postmenopausal women[64] and up to 36 folds more extensive than that of osteoporosis on the ground[32, 33].

Currently, there is no FDA approved osteoporosis therapy for a long-term use with a combined osteogenic and anti-resorptive property. Such therapy is in dire need particularly for extreme cases of bone loss such as osteoporosis complicated by disuse atrophy and spaceflight-induced osteoporosis[65]. Numerous studies have shown the involvement of Wnt/β-catenin pathway in reducing osteoblastogenesis and osteoclastogenesis in the microgravity settings, leading to a rapid bone loss[35, 64, 66]. Preliminary studies suggest that NELL-1 also exerts a systemic, protective function against osteoporotic bone loss via modulating both osteoblast (OB) and osteoclast (OC) activity[62, 67, 68]. One of the first clues to the integral role of NELL-1 signaling in the balance of OB versus OC activity came from the isolation of NELL-1 deficient cells[54, 62]. Bone marrow stromal cells (BMSC) isolated from Nell-1 haploinsufficient mice showed marked impairment in osteogenesis and pre-osteoclasts showed inappropriate activation, leading to increased number, size, and depth of resorption pits[62]. On the other hand, osteoprogenitor cells cultured from Nell-1+/- mice showed increased proliferation and differentiation[62]. Subsequent studies have continued to verify the properties of NELL-1 as a Wnt/β-catenin regulator that acts on both anabolic (pro-

osteoblastic) and antiosteoclastic[62, 68-70]. With these findings, we anticipate that NELL-1 as a positive Wnt/β-catenin regulator will provide a new strategy as a dual-function therapy for treating bone loss in the space and on Earth.

1.6 PEGylation of NELL-1

PEGylation is an FDA approved method to enhance the bioavailability of the protein for systemic application[71]. Excitingly, PEGylation of NELL-1 (NELL-PEG) remarkably enhances its plasma half-life and systemic pharmacokinetics[68], extending the dosing interval from two days (q2d) to q7d, and even q14d to meet the technical demands of our ongoing NASA spaceflight study, supporting its clinical use. With PEGylation, the half-life of NELL-1 was increased by up to 6 folds without any considerable toxicity to the vital organs[67, 68].

1.7 Conjugation of NELL-PEG with inactive bisphosphonate (BP)

The RR-5 mission with NASA demanded a reduced dosing frequency to at least every-14-days (q14d) because astronauts could only access the animals every 2 weeks onboard the ISS National Lab. As such, we had engineered NELL-1 to increase target-specificity to add retention in bone tissues. We have conjugated NELL-PEG with inactive BP (alendronate), thereby increasing protein uptake by bone. Using BP as a bone seeking molecule is a highly investigated method in the field of medical pharmacology[25, 72-76]. Even when BP is used in a minute amount at a non-therapeutic dose, it still retains the bone seeking property and creates a reservoir of BP conjugated drug on the bone surface[25, 72-76]. As OC resorbs the bone, the drug is released, binds to the receptors of OB and promotes bone formation.

For this study, the MW of BP and NELL-1 were 250 Da and 400 KDa, respectively, and they were conjugated at a ratio of 3:1. For treatment groups, 10mg/kg of BP-NELL-PEG was intraperitoneally injected every 2 weeks. This dosage of BP-NELL-PEG contained 75ug/kg of

conjugated BP: a negligible amount which is well below pharmacological dose. In addition, protein conjugation on the nitrogen of BP inactivates the BP molecule and removes its anti-OC function. Confirmation was done by the use of BP-BSA (Bovine Serum Albumin protein) as control, which was intravenously (IV) injected into mice. Interestingly, BP conjugation also allowed a significant deposition of NELL-1 in the craniofacial bone for the first time, as shown in the biodistribution data on NELL-1 vs. NELL-PEG vs. BP-NELL-PEG at 48hrs post-IV injection. As such, BP-NELL-PEG is expected to demonstrate more potent effects than either NELL-1 or NELL-PEG in craniofacial bones.

Our hypothetical model for BP-NELL-PEG's mechanism of action incorporates BP's strong bone affinity and NELL-PEG's osteogenic stimulation[82]. First, a reservoir of BP-NELL-PEG is formed on remodeling bone surface via BP's high bone-affinity as a pyrophosphate analog—binding to HA by electrostatic interaction with BP's phosphonate groups. Then, as OC resorb the bone, BP-NELL-PEG is released and binds to OB receptors, promoting bone formation. Some molecules are thought to be ingested by OC while others are degraded by lysosomes and eventually released as free particles in the extracellular matrix. NELL-1 is deemed to have an advantage over other protein drugs (e.i. BMP2, 26kDa) because its molecular mass (400 kDa) allows it to withstand several surface modifications without notably affecting bioactivity[67]. Also, even with PEGylation and inactive-BP conjugation, the protein (in nano scale) is significantly smaller than the diameter of capillaries (through which red cells of 6-8 micrometer diameter travel) and allows systemic administration.

2. MATERIALS AND METHODS

All experimental procedures followed the guidelines of the Chancellor's Animal Research Committee at UCLA and NASA Institutional Animal Care and Use Committees (IACUC). The

mice housed at UCLA were in pathogen-free ventilated cages, in a light and temperature-controlled environment, and had food and water ad libitum.

This study is a branch of the Rodent Research-5 mission and analysis was conducted on 40 32-week-old female BALB/c mice (Taconic Biosciences, NY). The age was selected based on a ground pilot study that revealed that female BALB/c mice attained their bone density plateau after 32 weeks.

Animals were housed at the Kennedy Space Station (KSC) 4 weeks before the mission and were randomly assigned into groups as shown in **Table 1**. This project focuses, for the first time, on the effects of space microgravity on the TMJ and treatment with BP-NELL-PEG.

On June 3rd, 2017, KSC-housed mice were transported to the ISS as part of SpaceX CRS-11. Starting week 1 and every other week thereafter, mice have received intraperitoneal injections with either PBS for BP-NELL-PEG (10mg/kg). The Ground Control groups were housed at KSC and matched exactly with the Flight groups. At the end of the mission (9 weeks long), mice returned to Earth and were euthanized and frozen. Carcasses were returned to UCLA for dissection and analyses.

In order to demonstrate that conjugated BP is inactivated, we performed a ground experiment using 4 BALB/c mice that matched the animals from our RR-5 mission. Rodents were injected four times, every other week, with 5.11mg/kg BP-bovine serum albumin (BP-BSA). The dose of BP matched the amount of BP used to conjugate the BP-NELL-PEG compound. This experiment serves as a control, as the conjugation method between BP and BSA was exactly the same as the BP-NELL-PEG conjugation. At the end of the study, mice were harvested, and analyses were performed using the same parameters.

Qualitative and quantitative analyses were performed on both microCT scans and histology images at the subchondral bone region and the corresponding covering cartilage.

2.1 Harvesting Procedure

All animals were euthanized by CO_2 (3L/min) displacement of oxygen, that continued for an additional minute after breathing stopped, followed by cervical dislocation. Each animal was carefully dissected to separate out different organs and the cranium was isolated for this project. All samples were fixated in 4% paraformaldehyde (PFA) for 48h and transferred to 70% ethanol thereafter.

2.2 Micro-CT Scan and Analysis

The mice craniums were scanned using micro-CT (SkyScan 1172; Bruker Micro-CT N.V.) at an image resolution of 10 um (55 kV and 181 mA radiation source, 0.5mm aluminum filter). Previously published methods[68] were followed for the micro-CT reconstruction and analysis. 3D images were reconstructed from the 2D X-ray projections by implementing the Feldkamp algorithm and appropriate image corrections, including ring artifact correction, beam hardening correction, and fine-tuning, were processed using NRecon software (SkyScan 1172, Belgium), with the same correction settings used for all scans regardless of experimental group. After acquisition and reconstruction of datasets, 3D morphometric analyses of the mandibular condyle and mandible were performed using CT-Analyzer software (SkyScan 1172, Belgium). First, images were reoriented to align the long axis of the mandibular condyle parallel to the coronal plane. The region of interest was then determined separately on the right mandibular condyle for each cranium, as is depicted in **Fig. 1**, in order to isolate the superior aspect of the condyle. We selected the following region of interest (ROI): the most convex points on the medial and lateral edges of the condyles were connected and the volume between this line and the superior surface

of the condyle was analyzed, as in **Fig. 1**. This was done by first roughly delimiting this region with the freehand tool (including soft tissues around the condyle), and then using the shrink-wrap tool in order to shrink the ROI to only the bony tissue of the condyle. In order to perform the shrink-wrap operation and calculate morphometric parameters, we set a threshold for bone of 75 to 255, based on qualitative analysis of the scanned images from all experimental groups at multiple threshold values. Specifically, the lower threshold was varied from 50-90 with the upper threshold held at 255, and the condyle was observed for how well each threshold (1) included as much bone tissue as possible while (2) excluding non-bony tissue, such as marrow within trabecular pores (**Fig. 2**). Morphometric parameters were then computed from the binarized images based on the threshold, using direct 3D techniques (marching cubes and sphere-fitting methods), and included bone mineral density (BMD, g/cm3), percent bone volume, or more accurately percentage absolute calcified tissue volume (BV/TV, %), trabecular number (Tb.N, mm^{-1}), trabecular thickness (Tb.Th, mm), trabecular separation (Tb.Sp, mm), and total porosity (Porosity, %). All quantitative and structural parameters followed the nomenclature and units recommended by the American Society for Bone and Mineral Research (ASBMR) Histomorphometry Nomenclature Committee[77].

Additionally, mandibular length measurements were performed according to the protocol published in Vora et. al[78] to assess whether there is a growth process at the condylar level with BP-NELL-PEG treatment. Additional measurements were included as depicted in **Fig. 3**.

2.3 Histology Analysis

After the completion of micro-CT, all samples were preserved in 70% ethanol before being processed for histology. Craniums were decalcified in 19% EDTA solution for 14 days, dehydrated, and processed for paraffin embedding. For consistency and accuracy, craniums were

dissected in two halves and positioned on a flat surface. The temporomandibular joint area was isolated using 90-degree cuts allowing the samples to be analyzed in coronal view. Five-micron thick sections were cut, and the slides were stained with Hematoxylin and Eosin (H&E), Masson's Trichrome, Safranin-O and Alcian Blue as per standard protocols. Histological specimens were analyzed using the Olympus BX51 microscopes and images were captured with Olympus DP73 digital camera and cellSens Imaging Software (Tokyo, Japan).

In addition to the qualitative histological analysis, we also developed a protocol to quantitatively assess the changes in length and morphology of the condyles on histology. Gross histomorphometric measurements were performed on the condylar head in the coronal plane at five different landmarks: medial-most, medial, median, lateral and lateral-most (**Fig. 4**). Additionally, cartilaginous layer thickness was measured for the articular, polymorphic, mature and hypertrophic zones.

To generate the landmarks for the histomorphometric measurements, a vertical line was drawn through the long axis of the condyle in the histology images. Horizontally, a line that delimitates the lower border of the condylar head was drawn (defined as the most convex point on the lower border of the condylar head). The angle formed by the two lines was bisected obtaining the medial and lateral landmarks. In addition, to obtain the landmarks for the layer measurements, a perpendicular line was drawn from the previously selected points, and quantification was carried out along the line. The layers were defined according to the morphology of the cells present in the area: articular zone contains flat cells, the polymorphic zone presents disorganized cells with nuclei in the center of the cell, the mature region presents hypertrophic cells with big centered nuclei, and the hypertrophic zone contains hypertrophic cells with small or no nuclei (**Fig. 5**).

2.4 Statistical Analysis

The Shapiro-Wilk test was applied prior to data analysis to assess the normality of the dataset for each experimental group. After the normality test revealed a Gaussian distribution for each dataset, two-way analysis of variance (2-way ANOVA) followed by the Tukey test were used to compare all the measurements. All tests were performed using GraphPad Prism (GraphPad Prism version 8.0.0 for MacOS, GraphPad Software, San Diego, California, USA). The baseline significance level was established at an alpha of 0.05, although many comparisons produced an alpha level of 0.01 or less. Significant differences are indicated with bars and asterisks (* for ≤0.05, ** for ≤ 0.01, *** for ≤0.001, and **** for ≤0.0001) or different letter labels (two groups with different letters indicate statistically significant difference; two groups with the same letter indicate nonsignificance).

3. RESULTS

3.1 Spaceflight Microgravity Induced TMJ-OA in the condyles

As previously mentioned, the diagnosis of TMJ-OA is mainly based on the radiographic changes seen at the condylar level. Among these changes include remodeling of subchondral bone with subsequent flattening of the condyles. Moreover, TMJ-OA is also characterized by cartilage degradation.

We hypothesized that spaceflight microgravity will lead to a reduced cartilage thickness and subchondral bone loss and remodeling. Comparing our ground and flight PBS groups (on microCT and histology) we can observe TMJ-OA like changes after 9 weeks of spaceflight (**Fig. 6**). Looking at the subchondral bone, microCT reveals condylar flattening and remodeling in the flight PBS group. BMD changes are not significant; however, BV/TV has increased, and porosity has decreased with flight. This finding is not surprising, as with the subchondral bone remodeling,

the superior portion on the condyles was lost and the remaining bone appears to be more compact. At the cartilage level, histomorphometric measurements show a slight decrease of the condylar cartilage after spaceflight, however the decrease is not statistically significant ($p<0.05$).

3.2 Qualitative Results

3.2.1 Bone Analysis Results

For the Flight PBS control, we observed increased subchondral bone resorption and surface irregularity in the condylar head compared to Ground PBS. We also noted increased red stained tissue in Flight PBS compared to Ground PBS. In the treatment groups, both Ground and Flight groups showed increased volume and convexity of the condylar bone towards the medial (histology; coronal sections) and posterior (microCT; sagittal sections) directions. Moreover, the red stained tissue was not observed in the condylar head in both treatment groups (**Fig. 7**).

3.2.2 Cartilage Analysis Results

We observed apparent but insignificant differences between the Ground PBS and Flight PBS groups. However, with BP-NELL-PEG treatment, there was a striking increase in hypertrophic and mature zones, with hypertrophic-like tissue encroaching down to the condylar neck. Despite the increased proliferation of cartilage, microCT findings showed that the area was highly mineralized with similar tissue density to bone (**Fig. 8**).

3.3 Quantitative Results

3.3.1 Bone Mineral Density (BMD)

BMD of the condyles was slightly increased in the BP-NELL-PEG groups compared to the PBS and BP-BSA groups, however the difference is not statistically significant ($p<0.05$) (**Fig. 9**). This result is consistent with the visual analysis presented in color scaled images and demonstrates that the tissue proliferation at the subchondral bone level has similar mineralization compared to

our control groups. Moreover, comparing the PBS and BP-BSA groups, the results indicate that the low dose of BP used in the conjugation of BP-NELL-PEG shows no difference in mineral density at the condylar level ($p<0.05$) (**Fig. 9**).

3.3.2 Bone Volume to Total Volume Ratio (BV/TV)

Regarding the bone volume to total volume ratio (BV/TV), both BP-NELL-PEG groups showed an increase compared to the BP-BSA and PBS groups ($p<0.05$) (**Fig. 9**). There is a statistically significant difference between the PBS and BP-BSA groups ($p<0.05$), indicating a potential osteodegenerative process in the BP-BSA group, and further confirming the inactivation of BP-BSA with conjugation. Overall, BV/TV results might indicate that there is an increased osteogenic activity in the BP-NELL-PEG treatment group compared to the BP-BSA and PBS groups.

3.3.3 Porosity (%)

Porosity analysis describes the measurement of "void fraction" and characterizes the empty spaces within bone. This parameter is highly correlated with the overall mechanical strength of the bone. In our study, porosity of the condyles significantly decreased in the BP-NELL-PEG groups compared to the BP-BSA and PBS groups, for both flight and ground mice (**Fig. 9**). There is also a significant difference between the BP-BSA and PBS groups ($p<0.05$), further confirming BP inactivation with conjugation. These results correlated with BMD and BV/TV indicate a potent net osteogenic effect in the BP-NELL-PEG treatment group.

3.3.4 Trabecular Number (Tb.N), Trabecular Thickness (Tb.Th.) and Trabecular Separation (Tb.Sp.)

8 weeks of total treatment resulted in a lower number of trabeculae in the BP-NELL-PEG groups compared to the BP-BSA and PBS groups ($p<0.05$), in addition to the decrease in porosity.

There is a statistically significant difference in trabecular number between BP-NELL-PEG and BP-BSA groups as well as between BP-NELL-PEG and PBS groups ($p<0.05$) (**Fig. 9**). There is also a statistically significant difference between BP-BSA and PBS groups ($p<0.05$).

Additionally, trabecular thickness has increased in the BP-NELL-PEG group compared to the BP-BSA groups and PBS groups ($p<0.05$) (**Fig. 9**). There is also statistically significant difference between the BP-BSA and PBS groups ($p<0.05$).

Finally, the BP-BSA had the highest trabecular separation compared to the BP-NELL-PEG groups and PBS groups ($p<0.05$) (**Fig. 9**).

All in all, the microCT results how no difference in BMD among groups, a higher BV/TV, lower, trabecular number and separation with BP-NELL-PEG treatment.

3.3.5 Mandibular Length Measurements Results

Length measurements were performed to assess whether there is a change in the mandibular length after 8 weeks of BP-NELL-PEG treatment on ground and spaceflight. Our results show a slight decrease with BP-NELL-PEG treatment in both Ground and Flight groups; however, the values are not statistically significant ($p<0.05$). These results indicate that the changes observed in the condyle are most likely attributed to bone remodeling processes and not due to growth (**Fig. 10**).

3.3.6 Histomorphometric Measurements Results

The gross morphological measurements were performed on histology images comparing the PBS and BP-NELL-PEG groups (both ground and flight). The results of the gross morphological analysis showed generally an increase in cartilage thickness with BP-NELL-PEG treatment (**Fig. 11**). The greatest and most statistically significant increase is in the radius of the condyle, between the flight PBS and flight BP-NELL-PEG groups at the medial and median

landmarks ($p<0.05$). There is no significant difference in the medial-most, lateral and lateral-most measurements.

In the layer analysis, we have characterized the cell zones according to their morphology. For the articular zone, we can observe a slight decrease in thickness with BP-NELL-PEG treatment in both ground and flight groups compared to the PBS control groups; however, the changes are not statistically significant ($p<0.05$) (**Fig. 12**). In the polymorphic zone, there is a decrease in values for the BP-NELL-PEG treatment groups compared to the ground PBS group. This finding might be attributed due to the increase in the mature and hypertrophic zones that would generate a compressive force on the polymorphic zone (**Fig. 12**). In the mature zone, the values are increased for the BP-NELL-PEG groups compared to the PBS control groups (for both ground and flight groups). The highest increase was 84% at the median landmark between the flight BPS and BP-NELL-PEG treatment ($p<0.05$) (**Fig. 12**). The most striking difference was located in the hypertrophic zone. In the treatment groups, this layer has increased on average by 386.66% compared to our PBS control groups. We are attributing these findings to the BP-NELL-PEG treatment's effect on the TMJ. There is a tremendous significance behind the hypertrophic zone increase, because this is the deepest cartilage layer in the condyle that will later transform into calcified cartilage and further on in bone, during the endochondral ossification process (**Fig. 13**).

4. DISCUSSIONS

For the first time in the literature, our study is focusing on the effects of the microgravity on the TMJ and potential treatment against TMJ-OA using BP-NELL-PEG therapy. TMJ is a non-weight-bearing joint which means that there will not be any changes in the load due to weightlessness. Therefore, the effects that we observe in the Flight PBS group are attributed to spaceflight microgravity.

9-week flight duration led to subchondral bone remodeling and flattening of the condyles. However, our samples did not show a decrease in BV/TV, Tb.Th and increase in Tb.Sp as reported by Jiang et. al[79]. We consider that spaceflight led to an unquantifiable amount of bone loss (as seen in **Fig. 6**), and in the remodeling process the outer portion of the subchondral bone that contained the highest number of porosities was lost. This generated a lower value in porosity and trabecular number.

Based on our results, BP-NELL-PEG therapy resulted in an increase of the mature and hypertrophic layers in the mouse mandibular condyle as seen in the histology figures. Interestingly, similar histological findings were reported in studies that focused on the effect of bisphosphonate (BP) treatment alone on the TMJ. Kimura et al.[80] described an increased condylar volume and significant proliferation and thickening of the cartilage layers for WT mice that were treated with alendronate as BP. However, the age of the animals used in this study was three months old (growing mice) compared to our adult mice, 10 months at the time of harvest. Moreover, the total amount of BP injected was about 40 times more (12.5 mg/kg/month versus 150 μg/kg/month in our study). A similar study carried out on growing mice (Kim et al.,2009)[81], has reported an increase of the hypertrophic zone following alendronate treatment. The total dose of alendronate that was used was 14 mg/kg/month, higher than a regular BP dose administered in vivo. There are significant differences between the afore-mentioned studies and ours in terms on animal age, dosage and treatment length. We consider that the changes observed in our BP-NELL-PEG treated mice are indeed a result of NELL-1, and not BP (Alendronate). The low amount of BP has no therapeutic effects on the TMJ as it was demonstrated in our microCT analysis. We have observed similar BMD values, as well as similar bony architecture in the PBS and BP-BSA groups at the condylar level. These results are consistent with the findings of Shi[82] on long bones. Additionally,

an in vitro experiment carried out by the same author using osteoclast cultures, showed that BP-NELL-PEG and NELL-PEG treatment demonstrated strong anti-osteoclastic effects, with no significance between groups. Moreover, there was no difference between the blank control and the BP-BSA culture, further demonstrating that the low dose of BP conjugated with BSA is inactivated and BP loses its anti-OC effects.

Besides the effects that we observed on the histology images, microCT showed similar BMD values in the BP-NELL-PEG groups as in the PBS and BP-BSA groups suggesting that the cartilaginous tissue proliferation presents the same mineralization as our controls. Moreover, BV/TV values also increased in the BP-NELL-PEG groups due to decreased percentage of porosities. Overall, the quality of the newly formed tissue is higher than our control groups and we consider this a positive finding. Further studies are required to test our conclusion.

5. CONCLUSIONS

Based on our results, two months of spaceflight microgravity resulted in increased surface irregularity and condylar flattening. Although the decrease in cartilage thickness was not statistically significant, based on the microCT and histology images, our animal model shows TMJ-OA-like characteristics.

BP-NELL-PEG treatment in both ground and flight groups led to increased subchondral bone volume and decreased the percentage of porosities. Moreover, the condylar shape post-treatment is more convex towards medial and posterior directions (as seen in microCT and histology images). Mandibular length measurements showed no difference among groups. Hence, we conclude that there is no growth at the mandibular level on skeletally mature mice, but a replacement process at the condylar level. Further studies are necessary to determine whether the changes are favorable.

Two months of spaceflight did not cause a significant change in the cartilage layers. However, BP-NELL-PEG treatment significantly increased the mature and hypertrophic zones of the cartilage, with calcified tissue with cartilage-like phenotype encroaching down to the condylar neck.

6. STUDY LIMITATIONS

Although we observe significant differences with BP-NELL-PEG treatment, we cannot conclude whether the effects are favorable or not. One of the biggest limitations of our study was the lack of cell culture from the cranium necessary for RNA sequencing and protein analyses. Our conclusions are solely based on morphometric and visual analyses. Moreover, there was no recovery period after the spaceflight. A recovery group would have helped observing the evolution of the mature and hypertrophic cartilage zones and would better support our conclusions. Nevertheless, our findings are very exciting and unfold several future directions in TMJ studies.

7. FUTURE DIRECTIONS

While this is the first study that focuses on the effects of microgravity on the TMJ as well as treatment with BP-NELL-PEG, further studies are necessary to validate our results. However, this would require another spaceflight mission and extremely high costs. Simulated microgravity using hindlimb suspension is a potential alternative to space microgravity, however the effects on the bone and cartilage are still controversial and might not mimic real microgravity with complete fidelity.

As we observed striking changes in our BP-NELL-PEG groups, we will need to investigate whether these effects are positive or negative when translated clinically. Immunohistochemistry analysis using bone and cartilage specific markers such as osteocalcin (OCN), receptor activator

of nuclear factor kappa-β ligand (RANKL), Collagen I, II and X, as well as tartrate-resistant acid phosphatase (TRAP) enzymatic activity will help interpreting our results.

Overall, our preliminary data suggesting a similar bone density, less porosities and higher condylar volume following BP-NELL-PEG treatment could potentially be a promising therapy against TMJ-OA.

FIGURES

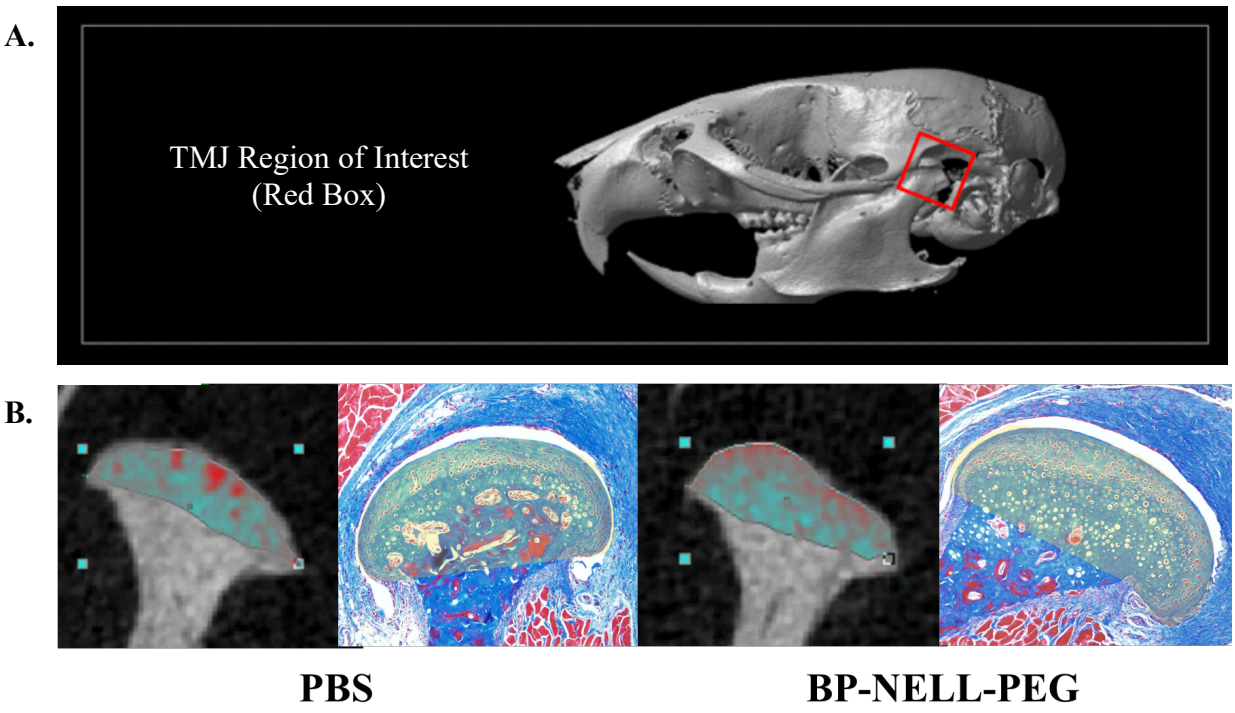

Figure 1. MicroCT Region of Interest (ROI) (A) Representative image of the rodent cranium on microCT and the TMJ region of interest, (B) Volume of interest (VOI) selection- representative microCT and histology images: the most medial and lateral points on the condylar head were connected and the volume between this line and the superior surface of the condyle was analyzed.

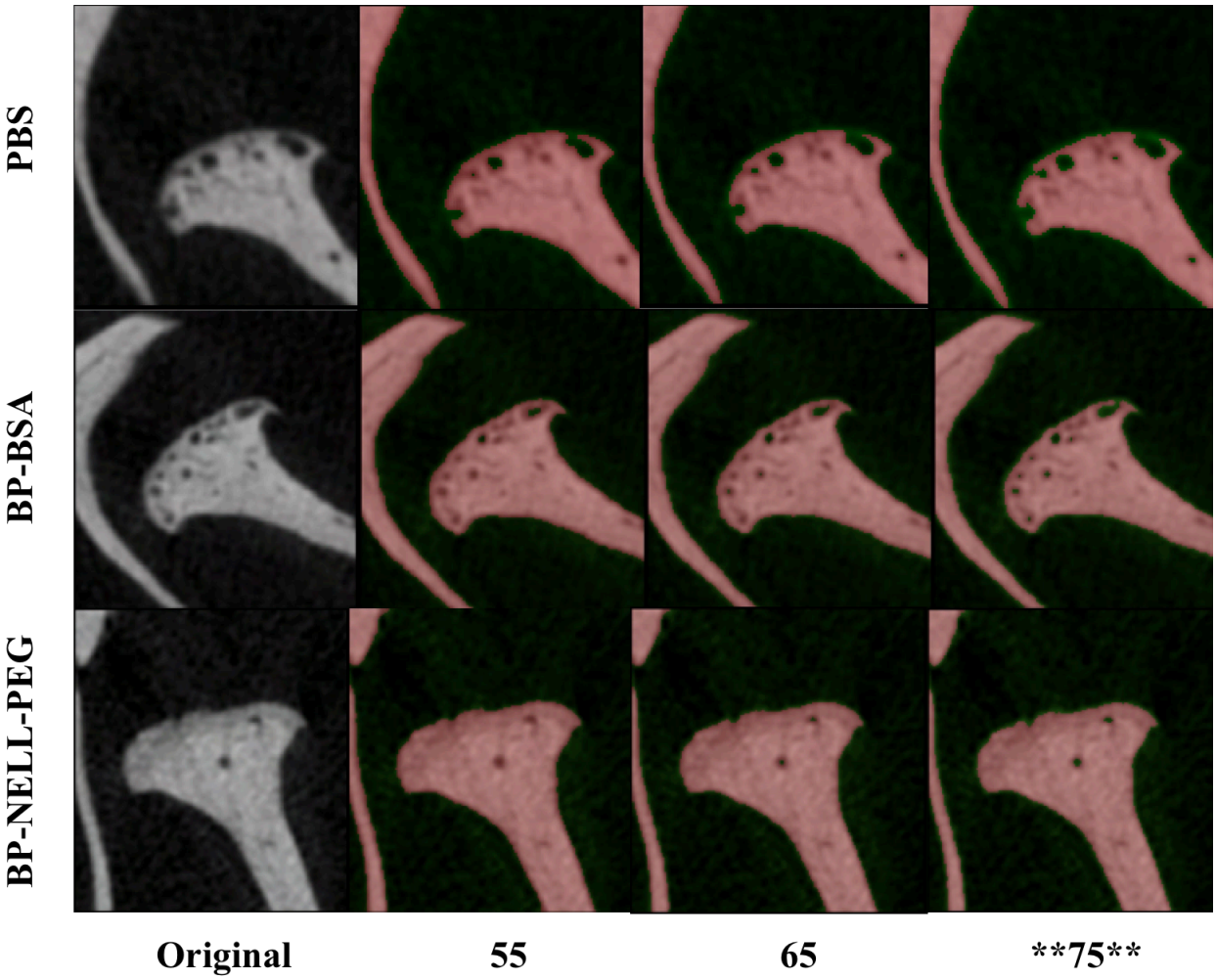

Figure 2. MicroCT threshold selection. The condyles were observed for how well each threshold (1) included as much bone tissue as possible while (2) excluding non-bony tissue, such as marrow within trabecular pores. All measurements were performed with a threshold of 75.

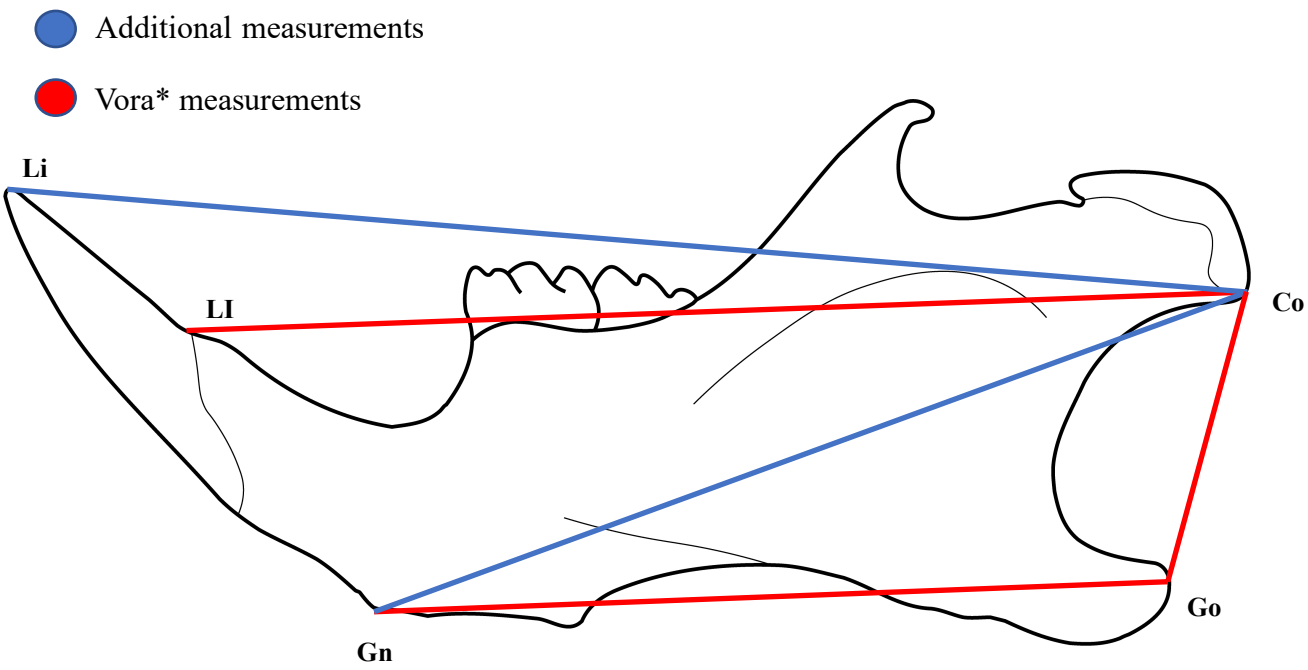

Figure 3. Mandibular length measurements landmarks. Mandibular length measurements were performed on microCT according to the landmarks presented in Vora et al.[78] (depicted in red lines) and additional measurements chosen by the authors (depicted in blue lines). Li=lower incisor tip, LI=lower incisor base, Gn=gnathion, Go=gonial process, Co=condylar process.

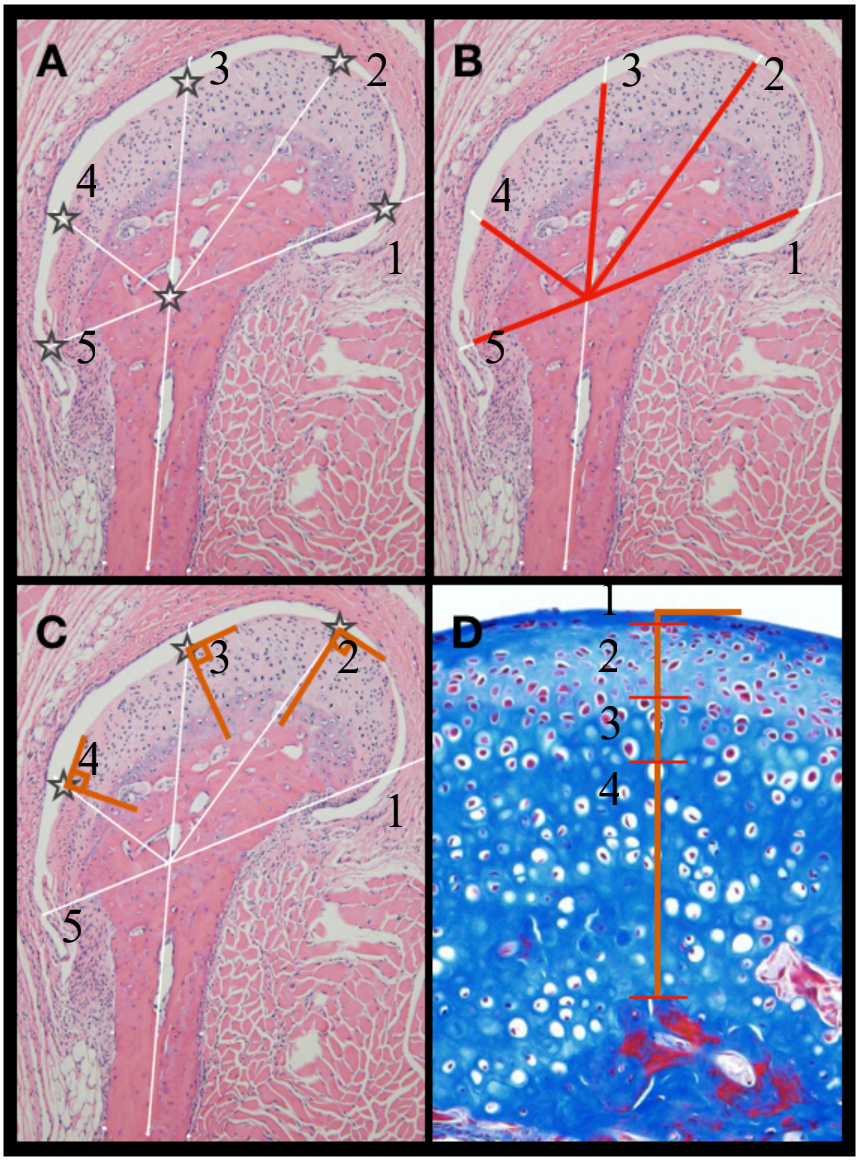

Figure 4. Histomorphometric measurements protocol. (A) To generate the landmarks for the histomorphometric measurements, a vertical line was drawn through the long axis of the condyle in the histology images. Horizontally, a line that delimitates the lower border of the condylar head was drawn (defined as the most convex point on the lower border of the condylar head). The angle formed by the two lines was bisected obtaining the medial and lateral landmarks, (B) Landmarks: 1-medial-most, 2-medial, 3-median, 4-lateral, 5-lateral-most, (C) To obtain the landmarks for the layer measurements, a perpendicular line was drawn from the previously selected points, and quantification was carried out along the line, (D) The layers were defined according to the morphology of the cells present in the area: 1-articular zone, 2-polymorphic zone, 3-mature zone, 4-hypertrophic zone.

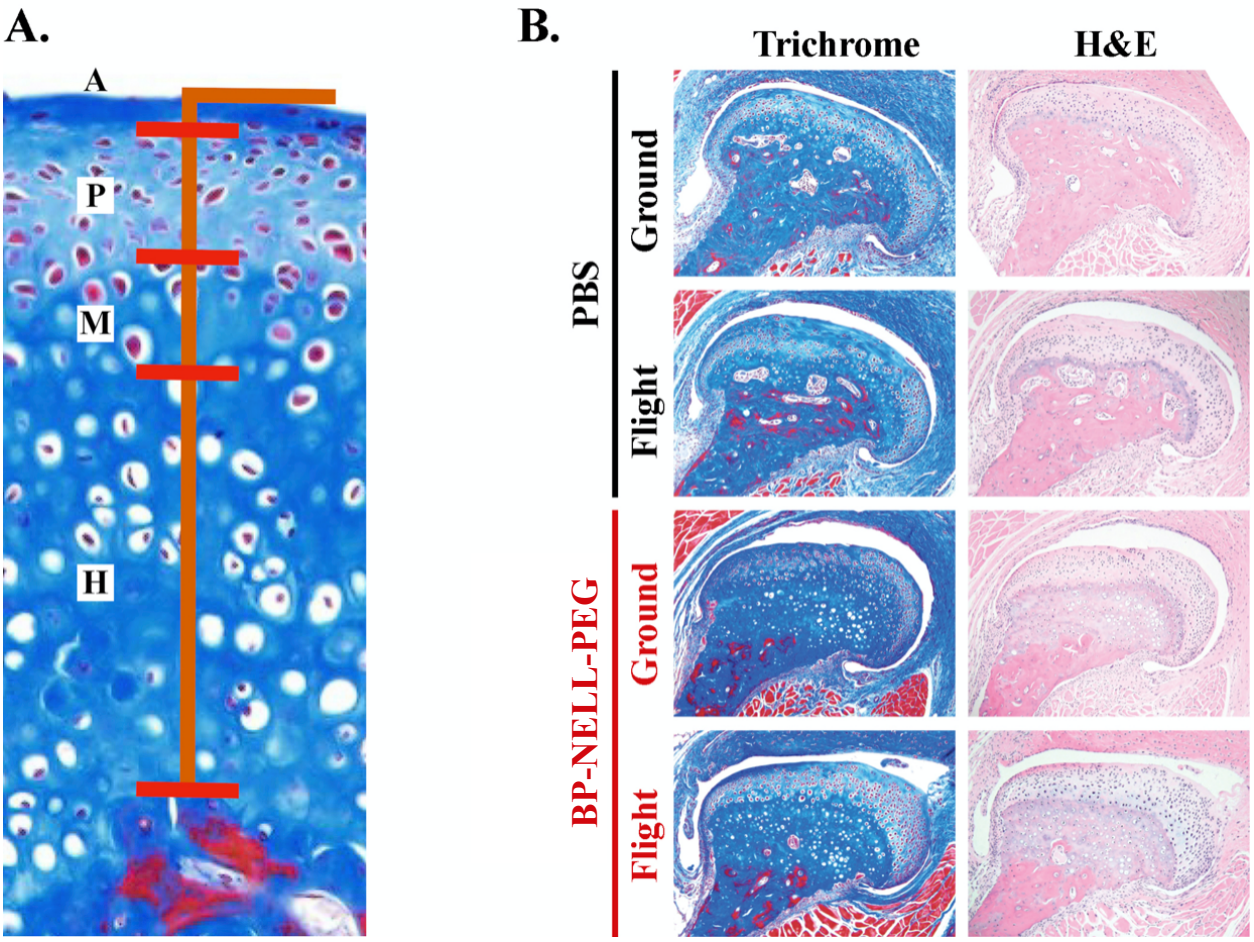

Figure 5. (A) **Histomorphometric layer analysis landmarks**. A=articular zone, P=polymorphic zone, M=mature zone, H=hypertrophic zone; (B) Representative histology images of the condyle in Masson's Trichrome and H&E staining. (*BP-NP=BP-NELL-PEG)

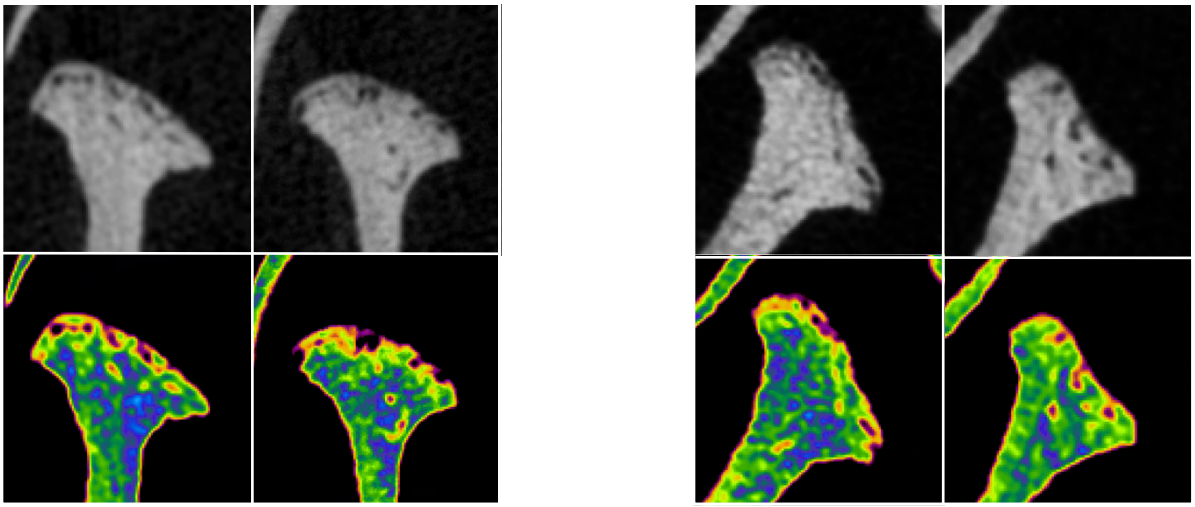

A. PBS Ground **B. PBS Flight**

Figure 6. Confirmation of TMJ-OA-like changes in the Flight PBS group. 8-week flight duration led to subchondral bone remodeling and flattening of the condyles. We consider that spaceflight led to an unquantifiable amount of bone loss, and in the remodeling process the outer portion of the subchondral bone that contained the highest number of porosities was lost. This generated a lower value in porosity and trabecular number.

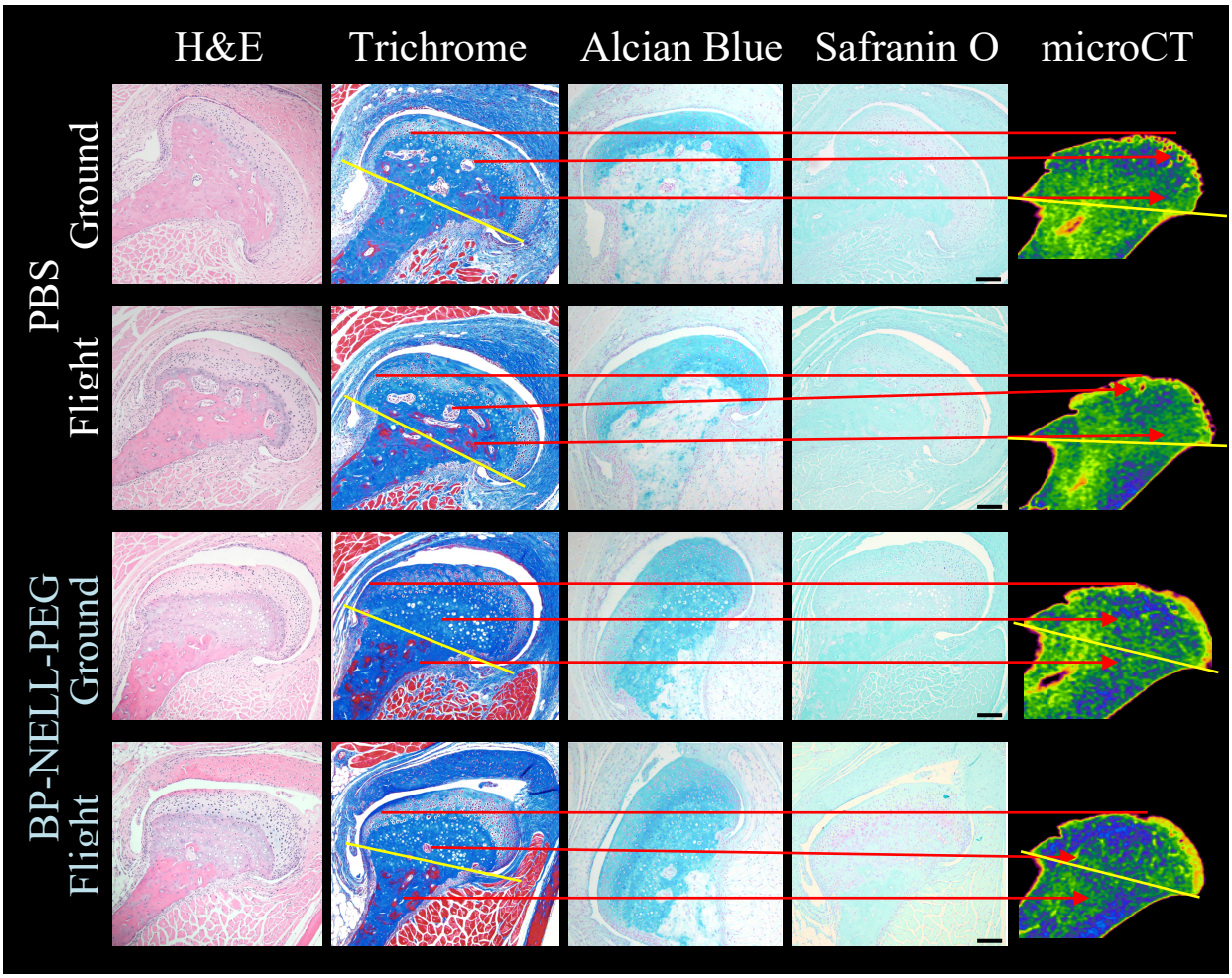

Figure 7. Bone analysis results (qualitative). We have performed histology analysis in bone-specific stains. In Flight PBS control, we observed increased subchondral bone resorption and surface irregularity in the condylar head compared to Ground PBS. We also noted increased red stained tissue in Flight PBS compared to Ground PBS. In the treatment groups, both Ground and Flight groups showed increased volume and convexity of the condylar bone towards medial (histology; coronal sections) and posterior (microCT; sagittal sections) direction. Moreover, the red stained tissue was not observed in the condylar head (above the yellow line on the Trichrome staining images) in both treatment groups.

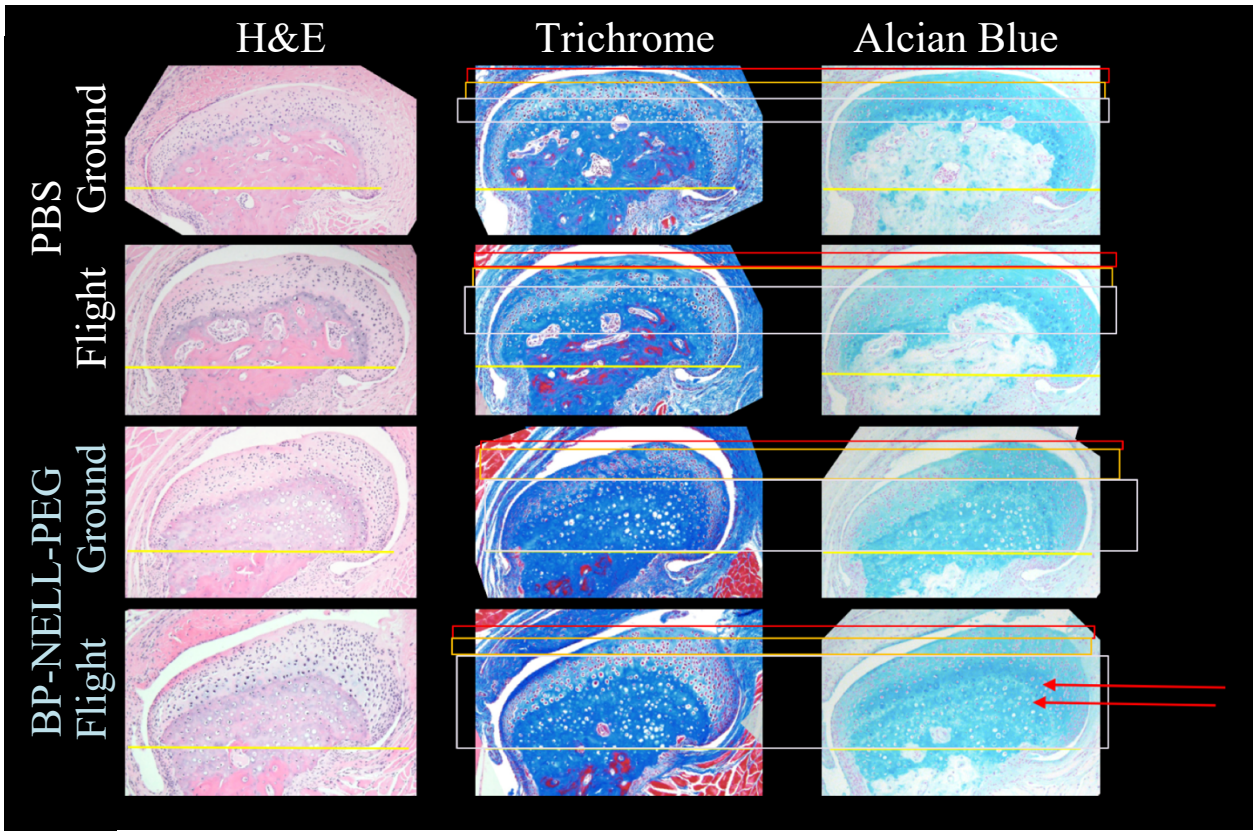

Figure 8. Cartilage analysis results (qualitative). The same H&E, Masson's Trichrome and Alcian Blue stains are reoriented/sized for better view of the cartilage component. Reference boxes (red box for articular + polymorphic zone; orange box for mature zone; and white box for hypertrophic zone) were included. We observed insignificant difference between Ground PBS and Flight PBS. However, with BP-NELL-PEG treatment, there was a strikingly increased hypertrophic and mature zones, with hypertrophic chondrocytes encroaching down to the condylar neck. Despite the increased proliferation of cartilage beyond therapeutic levels, microCT findings showed increased mineralization of the area.

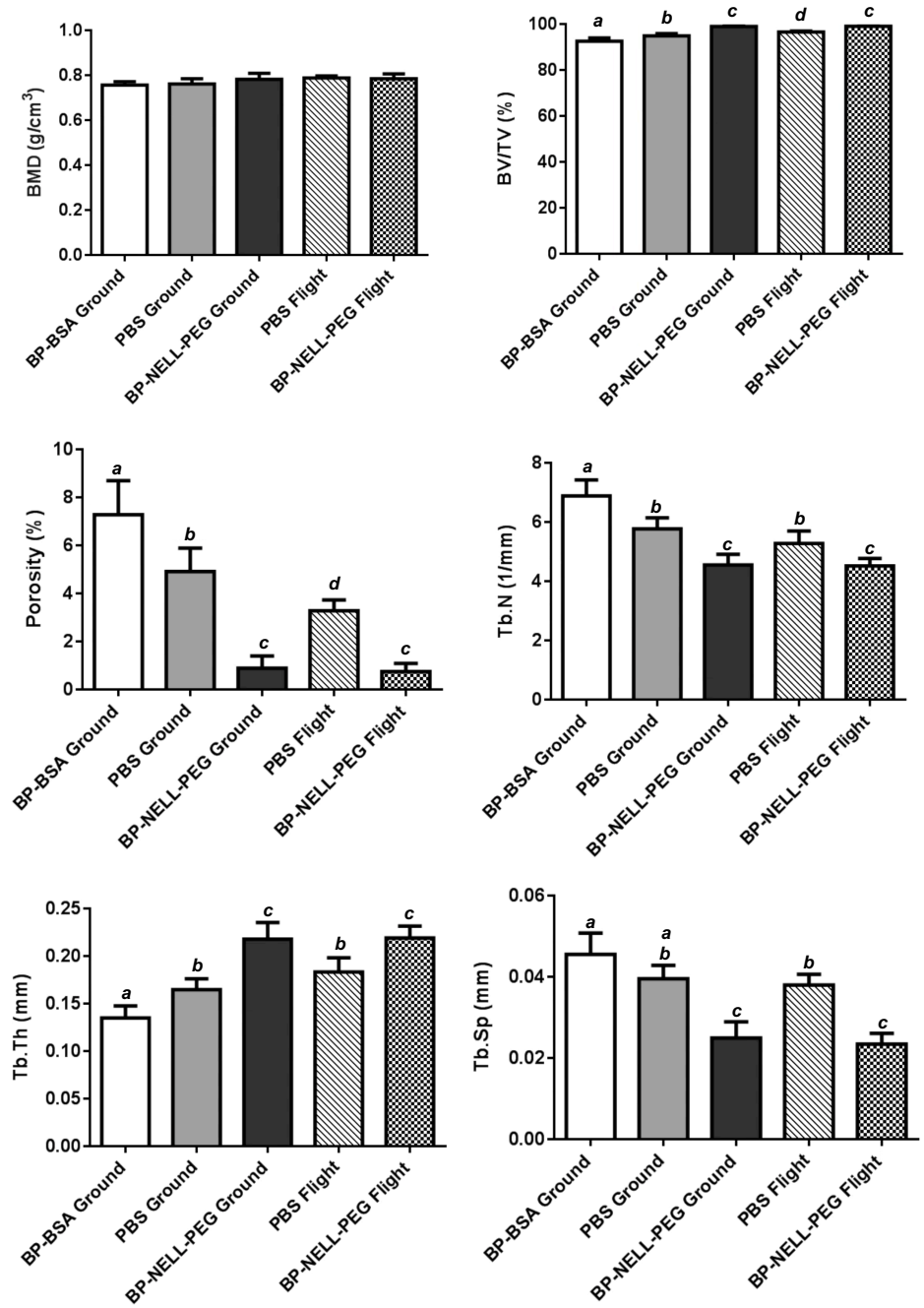

Figure 9. MicroCT results for PBS, BP-BSA and BP-NELL-PEG groups. Different lowercase letters indicate significant differences among groups. Significance level $p<0.05$.

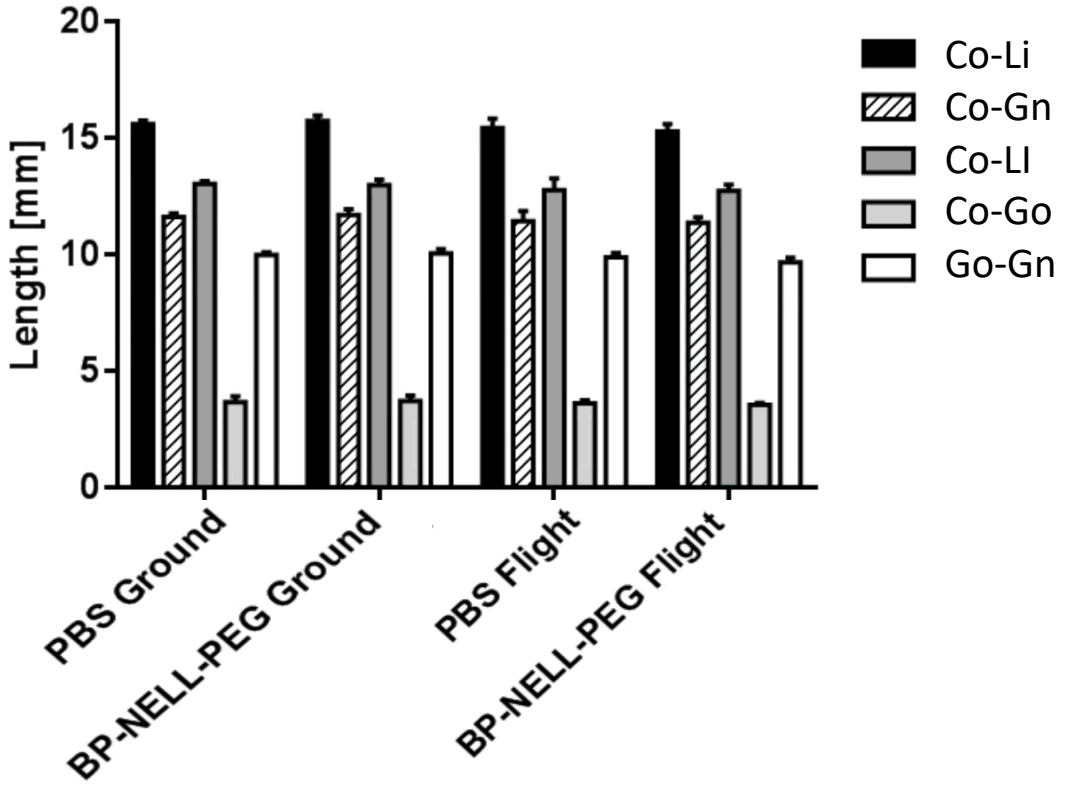

Figure 10. Mandibular length measurements results. Length measurements were performed on the microCT to determine whether we can observe any growth in skeletally mature mice. Our results show no difference among groups, concluding that our microCT and histology findings are caused by bone remodeling at the condylar level.

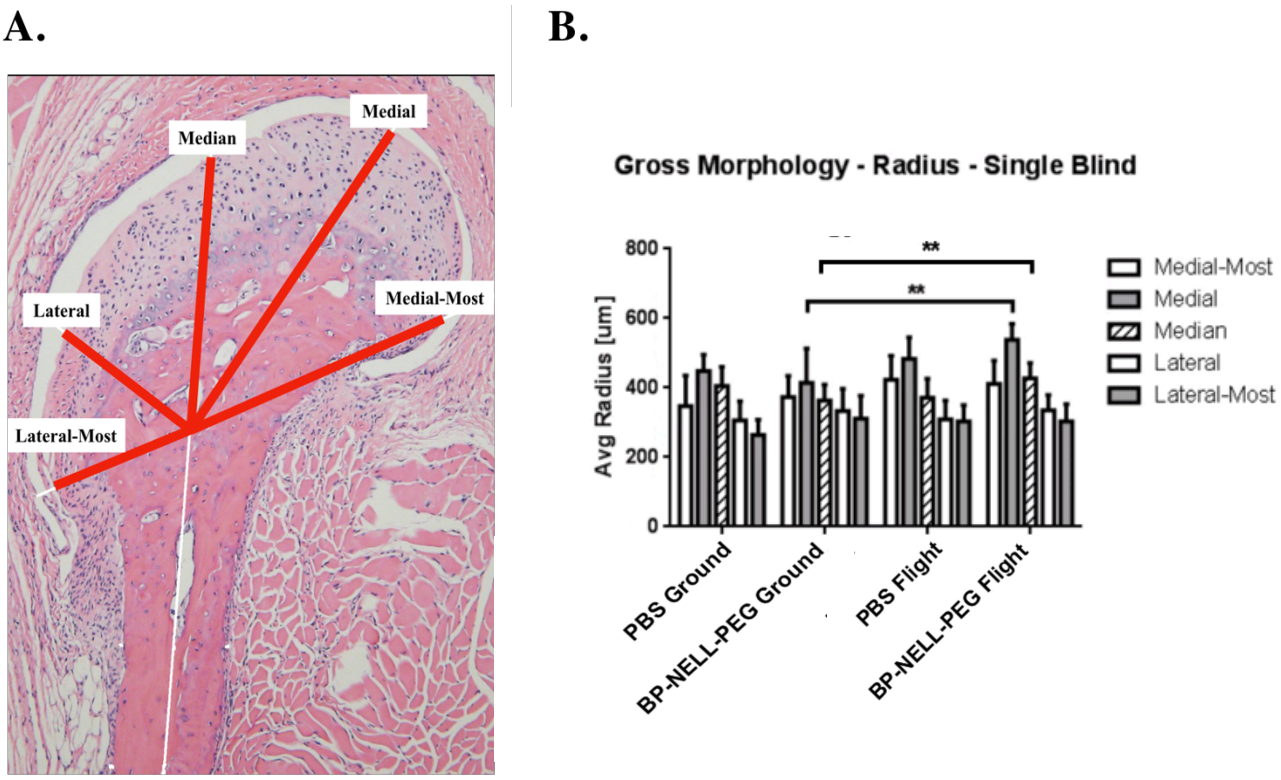

Figure 11. Histomorphometric analysis results. Single-blind measurements of cartilage zone thickness. (A) Labelled radial measurements on histology coronal section. (B) Interestingly, histological measurements show that BP-NP treatment contributed to statistically significant medial and upwards condylar remodeling in the 10-month-old skeletally mature mice. Measurements were completed on H&E and Masson's Trichrome stains by one examiner based on a prewritten protocol and standardized landmarks. Histology completed bilaterally and all results are consistent. (** $p \leq 0.01$)

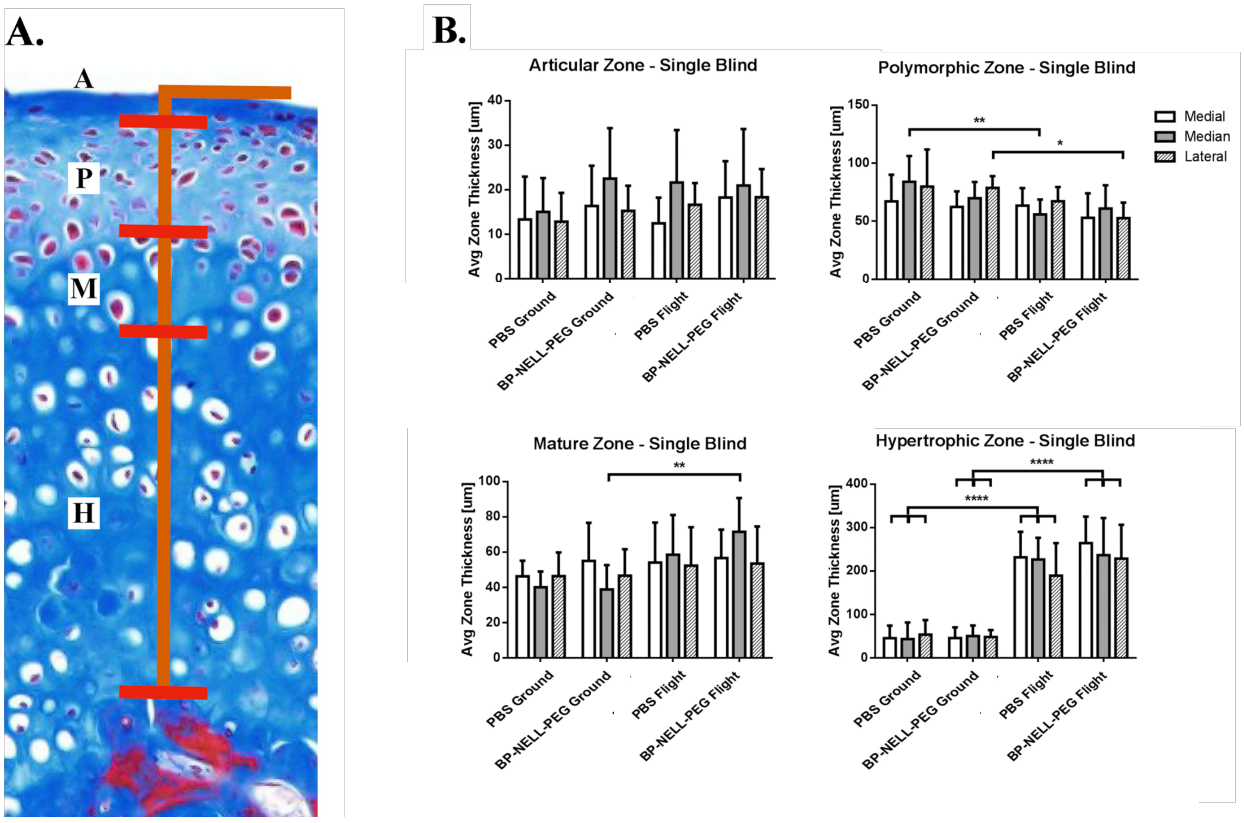

Figure 12. Histomorphometric layer analysis results. Single-blind measurements of cartilage zone thickness. (A) Cartilaginous zones include A = Articular zone, P = Polymorphic zone, M = Mature zone, H = Hypertrophic zone. Measurements were completed as shown on H&E and Masson's Trichrome stains, at medial, median, and lateral landmarks on the articular surface. (B) Strikingly, we observed a 3-fold increase in thickness of the calcified hypertrophic zone in BP-NELL-PEG treatment groups, in both Ground and Flight groups. Treatment also resulted in a statistically significant decrease in polymorphic zone thickness, within Ground and Flight groups. Histology completed bilaterally. (* $p \leq 0.05$, ** $p \leq 0.01$, *** $p \leq 0.001$, and **** $p \leq 0.0001$).

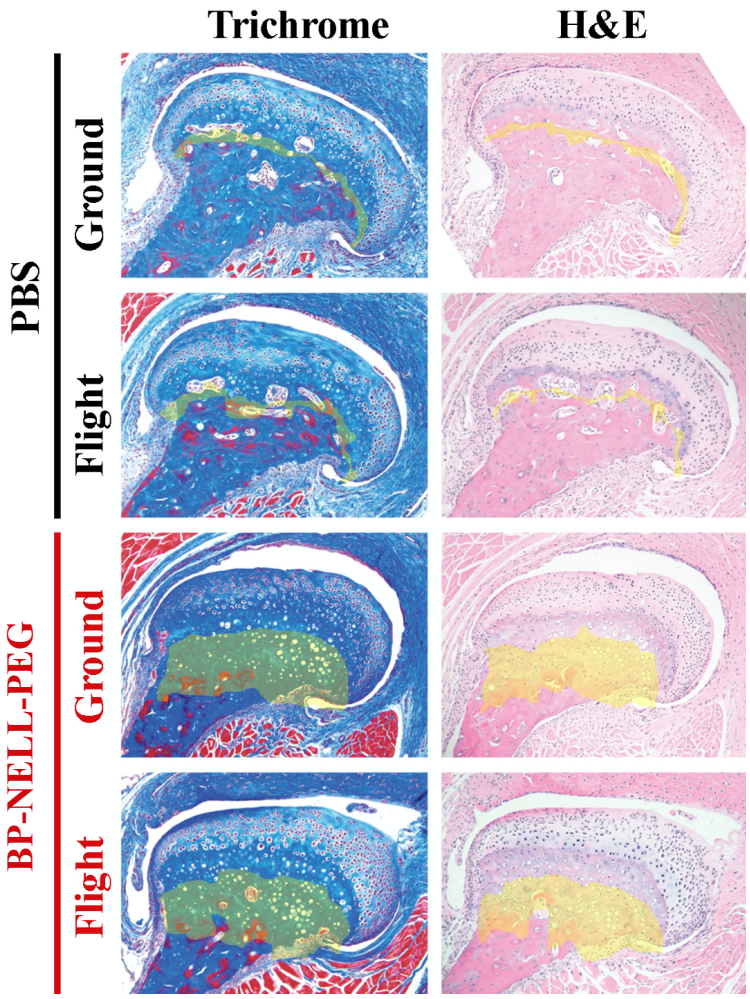

Figure 13. Representative histology images with approximately labelled hypertrophic zone. Highlighted hypertrophic zone displays a striking increase in thickness in BP-NELL-PEG treatment groups. Condyle morphology is also visibly altered with treatment, with increased volume and convexity of the condyle in the medial direction. All condyles showed similar trends.

RODENT RESEARCH-5 MISSION ANIMALS			
Group	Flight duration	Treatment	Animal #
Flight	9 weeks	BP-NELL-PEG	10
		PBS Control	10
	4 weeks (Live-return)	BP-NELL-PEG	10
		PBS Control	10
Ground	9 weeks	BP-NELL-PEG	10
		PBS Control	10
	4 weeks (Live-return)	BP-NELL-PEG	10
		PBS Control	10
Baseline			20
Total			100

ANIMALS USED FOR THIS STUDY			
Group	Flight duration	Treatment	Animal #
Flight	9 weeks	BP-NELL-PEG	10
		PBS Control	10
Ground	9 weeks	BP-NELL-PEG	10
		PBS Control	10
Total			40

Table 1. Experimental groups. The total number of the NASA Rodent Research-5 mission was 100, however the study included another group (Live return) that was not analyzed in our study. We have used the animals that were on the spaceflight mission for the full duration of the flight (n=40). Additionally, we used 4 8-months old BALB/c mice that were treated with BP-BSA serving as controls for the BP inactivation.

REFERENCES

1. Berry SD, Kiel DP, Donaldson MG, et al. Application of the National Osteoporosis Foundation Guidelines to postmenopausal women and men: the Framingham Osteoporosis Study. *Osteoporos Int*. Jan 2010;21(1):53-60. doi:10.1007/s00198-009-1127-3

2. Heinemann DF. Osteoporosis. An overview of the National Osteoporosis Foundation clinical practice guide. *Geriatrics*. May 2000;55(5):31-6; quiz 39.

3. Shuler FD, Conjeski J, Kendall D, Salava J. Understanding the burden of osteoporosis and use of the World Health Organization FRAX. *Orthopedics*. Sep 2012;35(9):798-805. doi:10.3928/01477447-20120822-12

4. Watts NB, Lewiecki EM, Miller PD, Baim S. National Osteoporosis Foundation 2008 Clinician's Guide to Prevention and Treatment of Osteoporosis and the World Health Organization Fracture Risk Assessment Tool (FRAX): what they mean to the bone densitometrist and bone technologist. *J Clin Densitom*. 2008 Oct-Dec 2008;11(4):473-7. doi:10.1016/j.jocd.2008.04.003

5. Czerwiński E, Badurski JE, Marcinowska-Suchowierska E, Osieleniec J. Current understanding of osteoporosis according to the position of the World Health Organization (WHO) and International Osteoporosis Foundation. *Ortop Traumatol Rehabil*. 2007 Jul-Aug 2007;9(4):337-56.

6. Jilka RL. Biology of the basic multicellular unit and the pathophysiology of osteoporosis. *Med Pediatr Oncol*. Sep 2003;41(3):182-5. doi:10.1002/mpo.10334

7. Pisani P, Renna MD, Conversano F, et al. Major osteoporotic fragility fractures: Risk factor updates and societal impact. *World J Orthop*. Mar 2016;7(3):171-81. doi:10.5312/wjo.v7.i3.171

8. Solomon DH, Johnston SS, Boytsov NN, McMorrow D, Lane JM, Krohn KD. Osteoporosis medication use after hip fracture in U.S. patients between 2002 and 2011. *J Bone Miner Res*. Sep 2014;29(9):1929-37. doi:10.1002/jbmr.2202

9. Lindsay R. The burden of osteoporosis: cost. *Am J Med*. Feb 1995;98(2A):9S-11S.

10. Kyrgidis A, Tzellos TG, Toulis K, Antoniades K. The facial skeleton in patients with osteoporosis: a field for disease signs and treatment complications. *J Osteoporos*. Feb 2011;2011:147689. doi:10.4061/2011/147689

11. Orrico SR, Giro G, Gonçalves D, Takayama L, Pereira RM. Influence of the period after ovariectomy on femoral and mandibular bone density and on induced periodontal disease. *J Periodontol*. Jan 2007;78(1):164-9. doi:10.1902/jop.2007.060136

12. Scheibel PC, Ramos AL, Iwaki LC. Is there correlation between alveolar and systemic bone density? *Dental Press J Orthod*. 2013 Sep-Oct 2013;18(5):78-83.

13. Vijay G, Chitroda PK, Katti G, Shahbaz S, Baba I, Bhuvaneshwari. Prediction of osteoporosis using dental radiographs and age in females. *J Midlife Health*. 2015 Apr-Jun 2015;6(2):70-5. doi:10.4103/0976-7800.158952

14. Jagur O, Kull M, Leibur E, et al. Relationship between radiographic changes in the temporomandibular joint and bone mineral density: a population based study. *Stomatologija*. 2011;13(2):42-8.

15. Ardakani FE, Mirmohamadi SJ. Osteoporosis and oral bone resorption: a review. *J Maxillofac Oral Surg*. Jun 2009;8(2):121-6. doi:10.1007/s12663-009-0030-y

16. Shi J, Lee S, Pan HC, et al. Association of Condylar Bone Quality with TMJ Osteoarthritis. *J Dent Res*. Jul 2017;96(8):888-894. doi:10.1177/0022034517707515

17. Nicolielo LFP, Jacobs R, Ali Albdour E, et al. Is oestrogen associated with mandibular condylar resorption? A systematic review. *Int J Oral Maxillofac Surg*. Nov 2017;46(11):1394-1402. doi:10.1016/j.ijom.2017.06.012

18. Maixner W, Diatchenko L, Dubner R, et al. Orofacial pain prospective evaluation and risk assessment study--the OPPERA study. *J Pain*. Nov 2011;12(11 Suppl):T4-11.e1-2. doi:10.1016/j.jpain.2011.08.002

19. Nilsson IM. Reliability, validity, incidence and impact of temporormandibular pain disorders in adolescents. *Swed Dent J Suppl*. 2007;(183):7-86.

20. Sato H, Osterberg T, Ahlqwist M, Carlsson GE, Gröndahl HG, Rubinstein B. Association between radiographic findings in the mandibular condyle and temporomandibular dysfunction in an elderly population. *Acta Odontol Scand*. Dec 1996;54(6):384-90. doi:10.3109/00016359609003556

21. Sena MF, Mesquita KS, Santos FR, Silva FW, Serrano KV. Prevalence of temporomandibular dysfunction in children and adolescents. *Rev Paul Pediatr*. Dec 2013;31(4):538-45. doi:10.1590/S0103-05822013000400018

22. Howard JA. Temporomandibular joint disorders in children. *Dent Clin North Am*. Jan 2013;57(1):99-127. doi:10.1016/j.cden.2012.10.001

23. Sampaio NM, Oliveira MC, Ortega AO, Santos LB, Alves TD. Temporomandibular disorders in elderly individuals: the influence of institutionalization and sociodemographic factors. *Codas*. Feb 2017;29(2):e20160114. doi:10.1590/2317-1782/20162016114

24. Hammarfjord O, Stassen LF. Bisphosphonate therapy and ankylosis of the temporomandibular joint: is there a relationship? A case report. *Oral Surg Oral Med Oral Pathol Oral Radiol*. Sep 2014;118(3):e68-70. doi:10.1016/j.oooo.2014.02.011

25. Skoglund K, Hjortdal O. Femoral fracture and temporomandibular joint destruction following the use of bisphosphonates. *Tidsskr Nor Laegeforen*. Jan 2015;135(2):116-7. doi:10.4045/tidsskr.14.1108

26. Kalra S, Jain V. Dental complications and management of patients on bisphosphonate therapy: A review article. *J Oral Biol Craniofac Res*. 2013 Jan-Apr 2013;3(1):25-30. doi:10.1016/j.jobcr.2012.11.001

27. Hamadeh IS, Ngwa BA, Gong Y. Drug induced osteonecrosis of the jaw. *Cancer Treat Rev*. May 2015;41(5):455-64. doi:10.1016/j.ctrv.2015.04.007

28. Diravidamani K, Sivalingam SK, Agarwal V. Drugs influencing orthodontic tooth movement: An overall review. *J Pharm Bioallied Sci*. Aug 2012;4(Suppl 2):S299-303. doi:10.4103/0975-7406.100278

29. Kanis JA, Johnell O, Oden A, et al. Long-term risk of osteoporotic fracture in Malmö. *Osteoporos Int*. 2000;11(8):669-74. doi:10.1007/s001980070064

30. Melton LJ, Atkinson EJ, O'Connor MK, O'Fallon WM, Riggs BL. Bone density and fracture risk in men. *J Bone Miner Res*. Dec 1998;13(12):1915-23. doi:10.1359/jbmr.1998.13.12.1915

31. Melton LJ, Chrischilles EA, Cooper C, Lane AW, Riggs BL. Perspective. How many women have osteoporosis? *J Bone Miner Res*. Sep 1992;7(9):1005-10. doi:10.1002/jbmr.5650070902

32. Lang T, Van Loon JJWA, Bloomfield S, et al. Towards human exploration of space: the THESEUS review series on muscle and bone research priorities. *NPJ Microgravity*. 2017;3:8. doi:10.1038/s41526-017-0013-0

33. Ohshima H. [Bone loss and bone metabolism in astronauts during long-duration space flight]. *Clin Calcium*. Jan 2006;16(1):81-5. doi:CliCa06018185

34. Di Giulio C. Do we age faster in absence of gravity? *Front Physiol*. 2013;4:134. doi:10.3389/fphys.2013.00134

35. Blaber EA, Finkelstein H, Dvorochkin N, et al. Microgravity Reduces the Differentiation and Regenerative Potential of Embryonic Stem Cells. *Stem Cells Dev*. Nov 2015;24(22):2605-21. doi:10.1089/scd.2015.0218

36. Blaber E, Sato K, Almeida EA. Stem cell health and tissue regeneration in microgravity. *Stem Cells Dev*. Dec 2014;23 Suppl 1:73-8. doi:10.1089/scd.2014.0408

37. Nabavi N, Khandani A, Camirand A, Harrison RE. Effects of microgravity on osteoclast bone resorption and osteoblast cytoskeletal organization and adhesion. *Bone*. Nov 2011;49(5):965-74. doi:10.1016/j.bone.2011.07.036

38. Ulbrich C, Wehland M, Pietsch J, et al. The impact of simulated and real microgravity on bone cells and mesenchymal stem cells. *Biomed Res Int*. 2014;2014:928507. doi:10.1155/2014/928507

39. Wadhwa S, Kapila S. TMJ disorders: future innovations in diagnostics and therapeutics. *J Dent Educ*. Aug 2008;72(8):930-47.

40. Benjamin M, Ralphs JR. Biology of fibrocartilage cells. *Int Rev Cytol*. 2004;233:1-45. doi:10.1016/S0074-7696(04)33001-9

41. Mizoguchi I, Nakamura M, Takahashi I, Kagayama M, Mitani H. A comparison of the immunohistochemical localization of type I and type II collagens in craniofacial cartilages of the rat. *Acta Anat (Basel)*. 1992;144(1):59-64. doi:10.1159/000147286

42. Milam SB. Pathogenesis of degenerative temporomandibular joint arthritides. *Odontology*. Sep 2005;93(1):7-15. doi:10.1007/s10266-005-0056-7

43. Symons NB. A histochemical study of the secondary cartilage of the mandibular condyle in the rat. *Arch Oral Biol*. 1965 Jul-Aug 1965;10(4):579-84. doi:10.1016/0003-9969(65)90003-8

44. Wang XD, Zhang JN, Gan YH, Zhou YH. Current understanding of pathogenesis and treatment of TMJ osteoarthritis. *J Dent Res*. May 2015;94(5):666-73. doi:10.1177/0022034515574770

45. Bäck K, Ahlqwist M, Hakeberg M, Björkelund C, Dahlström L. Relation between osteoporosis and radiographic and clinical signs of osteoarthritis/arthrosis in the temporomandibular joint: a population-based, cross-sectional study in an older Swedish population. *Gerodontology*. Jun 2017;34(2):187-194. doi:10.1111/ger.12245

46. Ting K, Vastardis H, Mulliken JB, et al. Human NELL-1 expressed in unilateral coronal synostosis. *J Bone Miner Res*. Jan 1999;14(1):80-9. doi:10.1359/jbmr.1999.14.1.80

47. Truong T, Zhang X, Pathmanathan D, Soo C, Ting K. Craniosynostosis-associated gene nell-1 is regulated by runx2. *J Bone Miner Res*. Jan 2007;22(1):7-18. doi:10.1359/jbmr.061012

48. Zhang X, Carpenter D, Bokui N, et al. Overexpression of Nell-1, a craniosynostosis-associated gene, induces apoptosis in osteoblasts during craniofacial development. *J Bone Miner Res*. Dec 2003;18(12):2126-34. doi:10.1359/jbmr.2003.18.12.2126

49. Zhang X, Cowan CM, Jiang X, et al. Nell-1 induces acrania-like cranioskeletal deformities during mouse embryonic development. *Lab Invest*. Jul 2006;86(7):633-44. doi:10.1038/labinvest.3700430

50. Zhang X, Kuroda S, Carpenter D, et al. Craniosynostosis in transgenic mice overexpressing Nell-1. *J Clin Invest*. Sep 2002;110(6):861-70. doi:10.1172/JCI15375

51. James AW, Pan A, Chiang M, et al. A new function of Nell-1 protein in repressing adipogenic differentiation. *Biochem Biophys Res Commun*. Jun 23 2011;doi:S0006-291X(11)01091-6 [pii]
10.1016/j.bbrc.2011.06.111

52. Pang S, Shen J, Liu Y, et al. Proliferation and osteogenic differentiation of mesenchymal stem cells induced by a short isoform of NELL-1. *Stem Cells*. Mar 2015;33(3):904-15. doi:10.1002/stem.1884

53. James AW, Pang S, Askarinam A, et al. Additive effects of sonic hedgehog and Nell-1 signaling in osteogenic versus adipogenic differentiation of human adipose-derived stromal cells. *Stem Cells Dev*. Aug 2012;21(12):2170-8. doi:10.1089/scd.2011.0461

54. Zhang X, Ting K, Bessette CM, et al. Nell-1, a key functional mediator of Runx2, partially rescues calvarial defects in Runx2(+/-) mice. *J Bone Miner Res*. Apr 2011;26(4):777-91. doi:10.1002/jbmr.267

55. Shen J, James AW, Chung J, et al. NELL-1 promotes cell adhesion and differentiation via Integrinβ1. *J Cell Biochem*. Dec 2012;113(12):3620-8. doi:10.1002/jcb.24253

56. Li W, Zara JN, Siu RK, et al. Nell-1 enhances bone regeneration in a rat critical-sized femoral segmental defect model. *Plast Reconstr Surg*. Feb 2011;127(2):580-7. doi:10.1097/PRS.0b013e3181fed5ae

57. Lu SS, Zhang X, Soo C, et al. The osteoinductive properties of Nell-1 in a rat spinal fusion model. *Spine J*. 2007 Jan-Feb 2007;7(1):50-60. doi:10.1016/j.spinee.2006.04.020

58. Li W, Lee M, Whang J, et al. Delivery of lyophilized Nell-1 in a rat spinal fusion model. *Tissue Eng Part A*. Sep 2010;16(9):2861-70. doi:10.1089/ten.tea.2009.0550

59. James AW, Shen J, Tsuei R, et al. NELL-1 induces Sca-1+ mesenchymal progenitor cell expansion in models of bone maintenance and repair. *JCI Insight*. Jun 2017;2(12)doi:10.1172/jci.insight.92573

60. Yuan W, James AW, Asatrian G, et al. NELL-1 based demineralized bone graft promotes rat spine fusion as compared to commercially available BMP-2 product. *J Orthop Sci*. Jul 2013;18(4):646-57. doi:10.1007/s00776-013-0390-5

61. Karasik D, Hsu YH, Zhou Y, Cupples LA, Kiel DP, Demissie S. Genome-wide pleiotropy of osteoporosis-related phenotypes: the Framingham Study. *J Bone Miner Res*. Jul 2010;25(7):1555-63. doi:10.1002/jbmr.38

62. James AW, Shen J, Zhang X, et al. NELL-1 in the treatment of osteoporotic bone loss. *Nat Commun*. Jun 2015;6:7362. doi:10.1038/ncomms8362

63. Kwak J, Zara JN, Chiang M, et al. NELL-1 injection maintains long-bone quantity and quality in an ovariectomy-induced osteoporotic senile rat model. *Tissue Eng Part A*. Feb 2013;19(3-4):426-36. doi:10.1089/ten.TEA.2012.0042

64. Grimm D, Grosse J, Wehland M, et al. The impact of microgravity on bone in humans. *Bone*. 06 2016;87:44-56. doi:10.1016/j.bone.2015.12.057

65. Cappellesso R, Nicole L, Guido A, Pizzol D. Spaceflight osteoporosis: current state and future perspective. *Endocr Regul*. Oct 2015;49(4):231-9. doi:10.4149/endo_2015_04_231

66. Lin C, Jiang X, Dai Z, et al. Sclerostin mediates bone response to mechanical unloading through antagonizing Wnt/beta-catenin signaling. *J Bone Miner Res*. Oct 2009;24(10):1651-61. doi:10.1359/jbmr.090411

67. Zhang Y, Velasco O, Zhang X, Ting K, Soo C, Wu BM. Bioactivity and circulation time of PEGylated NELL-1 in mice and the potential for osteoporosis therapy. *Biomaterials*. Aug 2014;35(24):6614-21. doi:10.1016/j.biomaterials.2014.04.061

68. Kwak JH, Zhang Y, Park J, et al. Pharmacokinetics and osteogenic potential of PEGylated NELL-1 in vivo after systemic administration. *Biomaterials*. Jul 2015;57:73-83. doi:10.1016/j.biomaterials.2015.03.063

69. Tanjaya J, Zhang Y, Lee S, et al. Efficacy of Intraperitoneal Administration of PEGylated NELL-1 for Bone Formation. *Biores Open Access*. 2016;5(1):159-70. doi:10.1089/biores.2016.0018

70. Shen J, James AW, Zhang X, et al. Novel Wnt Regulator NEL-Like Molecule-1 Antagonizes Adipogenesis and Augments Osteogenesis Induced by Bone Morphogenetic Protein 2. *Am J Pathol*. Feb 2016;186(2):419-34. doi:10.1016/j.ajpath.2015.10.011

71. Harris JM, Chess RB. Effect of pegylation on pharmaceuticals. *Nat Rev Drug Discov*. Mar 2003;2(3):214-21. doi:10.1038/nrd1033

72. Iannitti T, Rosini S, Lodi D, Frediani B, Rottigni V, Palmieri B. Bisphosphonates: focus on inflammation and bone loss. *Am J Ther*. May 2012;19(3):228-46. doi:10.1097/MJT.0b013e318247148f

73. Kennel KA, Drake MT. Adverse effects of bisphosphonates: implications for osteoporosis management. *Mayo Clin Proc*. Jul 2009;84(7):632-7; quiz 638. doi:10.1016/S0025-6196(11)60752-0

74. Lewiecki EM. Bisphosphonates for the treatment of osteoporosis: insights for clinicians. *Ther Adv Chronic Dis*. May 2010;1(3):115-28. doi:10.1177/2040622310374783

75. Neville-Webbe HL, Holen I, Coleman RE. The anti-tumour activity of bisphosphonates. *Cancer Treat Rev*. Dec 2002;28(6):305-19.

76. Shah NP, Nayee S, Pazianas M, Sproat C. Beyond ONJ - A review of the potential uses of bisphosphonates in dentistry. *Br Dent J*. May 2017;222(9):727-730. doi:10.1038/sj.bdj.2017.412

77. Parfitt AM, Drezner MK, Glorieux FH, et al. Bone histomorphometry: standardization of nomenclature, symbols, and units. Report of the ASBMR Histomorphometry Nomenclature Committee. *J Bone Miner Res*. Dec 1987;2(6):595-610. doi:10.1002/jbmr.5650020617

78. Vora SR, Camci ED, Cox TC. Postnatal Ontogeny of the Cranial Base and Craniofacial Skeleton in Male C57BL/6J Mice: A Reference Standard for Quantitative Analysis. *Front Physiol*. 2015;6:417. doi:10.3389/fphys.2015.00417

79. Jiang L, Shen X, Wei L, Zhou Q, Gao Y. Effects of bisphosphonates on mandibular condyle of ovariectomized osteoporotic rats using micro-ct and histomorphometric analysis. *J Oral Pathol Med*. May 2017;46(5):398-404. doi:10.1111/jop.12499

80. Kimura M, Miyazawa K, Tabuchi M, Maeda H, Kameyama Y, Goto S. Bisphosphonate treatment increases the size of the mandibular condyle and normalizes growth of the mandibular ramus in osteoprotegerin-deficient mice. *Calcif Tissue Int*. Feb 2008;82(2):137-47. doi:10.1007/s00223-007-9097-y

81. Kim MS, Jung SY, Kang JH, et al. Effects of bisphosphonate on the endochondral bone formation of the mandibular condyle. *Anat Histol Embryol*. Oct 2009;38(5):321-6. doi:10.1111/j.1439-0264.2009.00938.x

82. Shi J. Systemic Therapy of Inactivated-Bisphosphonate-Conjugated PEGylated NELL-1 (BP-NELL-PEG) for Spaceflight-Induced Osteoporosis. Doctor of Philosophy Dissertation 2019. Retrieved from https://escholarship.org/uc/item/0bk9h299